



Mitochondrial Alterations (Inhibition of Mitochondrial Protein Expression, Oxidative Metabolism, and Ultrastructure) Induced by Linezolid and Tedizolid at Clinically Relevant Concentrations in Cultured Human HL-60 Promyelocytes and THP-1 Monocytes

Tamara V. Milosevic,^a Valéry L. Payen,^b Pierre Sonveaux,^b Giulio G. Muccioli,^c  Paul M. Tulkens,^a  Françoise Van Bambeke^a

^aPharmacologie Cellulaire et Moléculaire, Louvain Drug Research Institute, Université catholique de Louvain, Brussels, Belgium

^bPole of Pharmacology, Institute of Experimental and Clinical Research, Université catholique de Louvain, Brussels, Belgium

^cBioanalysis and Pharmacology of Bioactive Lipids Research Group, Louvain Drug Research Institute, Université catholique de Louvain, Brussels, Belgium

ABSTRACT Linezolid, the first clinically available oxazolidinone antibiotic, causes potentially severe toxicities (myelosuppression, lactic acidosis, and neuropathies) ascribed to impairment of mitochondrial protein synthesis and consecutive mitochondrial dysfunction. Tedizolid, a newly approved oxazolidinone, shows an enhanced activity compared to linezolid but is also a more potent inhibitor of mitochondrial protein synthesis. We compared linezolid and tedizolid for (i) inhibition of the expression of subunit I of cytochrome *c*-oxidase (CYTox I; Western blot analysis), (ii) cytochrome *c*-oxidase activity (biochemical assay), (iii) mitochondrial oxidative metabolism (Seahorse technology), and (iv) alteration of mitochondrial ultrastructure (electron microscopy) using HL-60 promyelocytes and THP-1 monocytes exposed to microbiologically (multiples of modal MIC against *Staphylococcus aureus*) and therapeutically ($C_{\min} - C_{\max}$) pertinent concentrations. Both drugs caused a rapid and complete (48 to 72 h) inhibition of CYTox I expression, cytochrome *c*-oxidase activity, and spare respiratory capacity, with conspicuous swelling of the mitochondrial matrix and loss of their cristae. Globally, tedizolid was a more potent inhibitor than linezolid. For both drugs, all effects were quickly (48 to 72 h) and fully reversible upon drug withdrawal. Using an alternation of exposure to and withdrawal from drug mimicking their approved schedule of administration (twice daily and once daily [qD] for linezolid and tedizolid, respectively), only partial inhibition of CYTox I expression was noted for up to 96 h. Thus, rapid reversal of toxic effects upon discontinuous administration may mitigate oxazolidinone toxicity. Since tedizolid is given qD, this may help to explain its reported lower preclinical and clinical toxicity.

KEYWORDS oxazolidinones, linezolid, tedizolid, mitochondria, mitochondrial proteins, electron transport chain, mitochondrial metabolism, mitochondrial respiration

Linezolid (LZD), the first clinically available oxazolidinone antibiotic, inhibits bacterial protein synthesis by binding to the 23S rRNA of the large ribosomal subunit, preventing the assembly of 30S and 50S ribosomal subunits and the formation of initiation complex (1, 2). This mode of action is distinct from that of most other currently used classes acting on bacterial ribosomes, decreasing the risk of cross-resistance (3). Linezolid has become over the years a valuable therapeutic option in

Received 2 August 2017 Returned for modification 5 September 2017 Accepted 10 December 2017

Accepted manuscript posted online 20 December 2017

Citation Milosevic TV, Payen VL, Sonveaux P, Muccioli GG, Tulkens PM, Van Bambeke F. 2018. Mitochondrial alterations (inhibition of mitochondrial protein expression, oxidative metabolism, and ultrastructure) induced by linezolid and tedizolid at clinically relevant concentrations in cultured human HL-60 promyelocytes and THP-1 monocytes. *Antimicrob Agents Chemother* 62:e01599-17. <https://doi.org/10.1128/AAC.01599-17>.

Copyright © 2018 American Society for Microbiology. All Rights Reserved.

Address correspondence to Françoise Van Bambeke, francoise.vanbambeke@uclouvain.be.

difficult-to-treat infections by Gram-positive microorganisms where hosts' comorbidities and bacterial resistance to other agents have become problematic (see, for example, references 4, 5, 6, 7, 8, and 9). However, linezolid usage is associated with variable incidences of potentially severe adverse reactions associated with myelosuppression (anemia and thrombocytopenia [10, 11]), major metabolic disturbances (lactic acidosis [12, 13]), and neuronal toxicities (peripheral and ophthalmic neuropathies [14]). These effects, which are most commonly seen upon prolonged use of linezolid (15) and/or in patients with sustained trough levels (16), have been suggested to result from impairment of mitochondrial protein synthesis and consecutive mitochondrial dysfunction (17, 18). Thus, eperezolid, an early but discontinued oxazolidinone, was shown to cause time- and concentration-dependent inhibition of cell proliferation associated with a decrease in mitochondrial cytochrome *c*-oxidase subunit I expression, providing the first direct demonstration of mitochondria as a target for the toxic effects of this class of drugs (19). This has been further rationalized by the high degree of homology between bacterial and mitochondrial ribosomes and the existence of common binding sites for oxazolidinones (20, 21), explaining why derivatives with different antibacterial potencies were reported to bind to mitochondrial rRNA and to inhibit mitochondrial protein synthesis *in vitro* in direct relation to their antimicrobial potency (22). This implies that the development of new oxazolidinones needs to take into account not only their intrinsic antibacterial activity (including against linezolid-resistant strains) but also their potential mitochondrial toxicity (23, 24).

Tedizolid (formerly known as DA7157, TR700, or torezolid), is a new methyltetrazolyl oxazolidinone with enhanced activity against Gram-positive cocci (including strains carrying mobile *cf*r methyltransferase that confers resistance to linezolid), owing to additional target site interactions (25, 26). However, it is also a more potent inhibitor of mitochondrial protein synthesis than linezolid *in vitro* (27). Assessment of the overall mitochondrial toxicity of oxazolidinones for potential translation into the clinics should, however, not be limited to mere *in vitro* potency comparisons but must also take into account the conditions in which the drugs are used clinically so as to include parameters that can modulate toxicity, such as schedules of administration and actual peak and trough concentrations observed in patients. In this context, tedizolid markedly differs from linezolid in its currently approved conditions of administration (28, 29) that command a lower daily dosage and a lesser frequent schedule (200 mg once daily [qD] versus 600 mg twice daily [BID]). The aims of the present study were to better document and compare the potentials of linezolid and tedizolid to inhibit the expression of subunit I of cytochrome *c*-oxidase (CYTox I), a protein encoded by the mitochondrial genome and to examine its impact on mitochondrial oxidative metabolism and morphology in cultured human cells when using concentrations pertinent of those observed in patients receiving conventional doses of these antibiotics. We used two established human cell lines representing distinct potential targets of oxazolidinone myelosuppressive toxicity, namely, (i) HL-60 promyelocytes, a leukemic cell line with commitment toward myeloid differentiation (30, 31), and (ii) THP-1 monocytes, a leukemic cell line more differentiated as phagocytes (32). We observed that tedizolid is a more potent mitochondrial inhibitor than linezolid. However, the inhibition exerted by both drugs on mitochondrial protein expression and metabolism can be fully reversed by drug withdrawal, suggesting a potential mitigation of toxic effects when drug concentrations fluctuate over time in patient serum. (These data have been presented in part at ASM Microbe 2017 [New Orleans, LA, 1 to 5 June 2017, poster Saturday 150, Session 189-AAID03] and the 55th Interscience Conference on Antimicrobial Agents and Chemotherapy and 25th International Congress of Chemotherapy [San Diego, CA, 17 to 21 September 2015, poster A574].)

RESULTS

Inhibition of the expression of CYTox I and of cytochrome *c*-oxidase activity by oxazolidinones in HL-60 promyelocytes. In a first series of experiments, we evaluated the expression of CYTox I (one of the 13 proteins of the mitochondrial respiratory chain

encoded by mitochondrial DNA [33]) in HL-60 promyelocytes incubated for 120 h with increasing total concentrations of linezolid (0.25 to 25 mg/liter) or tedizolid (0.05 to 5 mg/liter). These concentrations were chosen to cover a range spanning from sub-MIC levels against *Staphylococcus aureus* (typical modal MICs as compiled by the European Committee on Antimicrobial Susceptibility Testing [EUCAST]: 2 mg/liter [linezolid] and 0.25 mg/liter [tedizolid] mg/liter [34]) to ~ 1.5 -fold their maximal total serum concentrations at equilibrium (C_{\max} , 15 mg/liter [linezolid] and 3 mg/liter [tedizolid]) commonly observed in patients receiving approved intravenous doses of these antibiotics (600 mg BID and 200 mg qD, respectively [28, 29, 35]). Expression of Tom 20, a protein of the outer mitochondrial membrane encoded by the nuclear genome, was evaluated in parallel for loading control purposes. As shown in Fig. 1A, both oxazolidinones caused a concentration-dependent decrease in the expression of CYTox I, and the protein became almost undetectable for drug concentrations greater than 15 and 0.25 mg/liter for linezolid and tedizolid, respectively. Tom 20 expression was unaffected. When the expressional ratio of CYTox I to Tom 20 was plotted against oxazolidinone concentrations expressed as multiples of their modal EUCAST MIC against *S. aureus*, tedizolid appeared to be ~ 6 -fold more inhibitory than linezolid (Fig. 1B; see caption for 50% inhibitory concentrations [IC_{50} s] in multiples of MIC, mg/liter, and μM).

Cytochrome *c*-oxidase activity was measured in parallel in lysates of cells subjected to the same treatments. Figure 1C shows that this activity was decreased in a concentration-dependent manner. Tedizolid was slightly more potent than linezolid, with an IC_{50} 1.6-fold lower than that of linezolid when concentrations were expressed as multiples of their modal EUCAST MIC against *S. aureus* (see caption for IC_{50} s in multiples of MIC, mg/liter, and μM). Figure 1D further shows a correlation between decreased cytochrome *c*-oxidase activity and reduced expression of CYTox I in these experiments. A significant correlation was seen for both oxazolidinones, but cytochrome *c*-oxidase activity decreased more rapidly with linezolid than with tedizolid for a similar decrease in CYTox I expression, illustrating differences in inhibitory potencies for CYTox I and cytochrome *c*-oxidase activity.

Influence of oxazolidinones on HL-60 promyelocytes proliferation and metabolic activity. In order to assess whether the effects described so far for CYTox I expression and cytochrome *c*-oxidase activity were the result of a general, nonspecific cytotoxicity of oxazolidinones or were specific of an effect on mitochondria, we evaluated the influence of both linezolid and tedizolid on cell proliferation (starting from an inoculum of 10^5 cells/ml) and their cytotoxicity (evaluated by their influence on metabolic activity) in HL-60 cells after 144 h of incubation over a wide range of concentrations. Results are shown in details in Fig. S1 in the supplemental material. Briefly, while the control cells population expanded by ~ 8 -fold in the 6-day period, linezolid and tedizolid decreased cell expansion in a concentration-dependent manner, with 50% inhibition achieved at $74\times$ the MIC for linezolid and $5\times$ the MIC for tedizolid. Conversely, cell toxicity (taking into account the difference in cell number) became apparent only at oxazolidinone concentrations of about $30\times$ their MICs, with maximal reductions of 48 and 34% at the highest concentrations tested ($200\times$ the MIC; 100 mg/liter [linezolid] and 50 mg/liter [tedizolid]).

Influence of the time of incubation with oxazolidinones on CYTox I expression and cytochrome *c*-oxidase activity in HL-60 promyelocytes and THP-1 monocytes. In the next series of experiments, we examined the changes of CYTox I expression over time in both HL-60 and THP-1 cells exposed to two selected concentrations of oxazolidinones (linezolid, 2.5 and 15 mg/liter; tedizolid, 0.5 and 3 mg/liter) corresponding to their respective human total C_{\min} and C_{\max} . The results are presented in Fig. 2, with images of the actual Western blots shown in the upper panels and quantitative data shown in the lower panels. At C_{\min} , linezolid only partially decreased CYTox I expression in HL-60 cells and was almost without effect in THP-1 cells. In contrast, the protein became undetectable after 48 h of incubation with tedizolid in HL-60 cells, and its expression was reduced in a time-dependent fashion in THP-1 cells, with only 29% of its original level being detected after 120 h. At C_{\max} , both oxazolidinones caused an

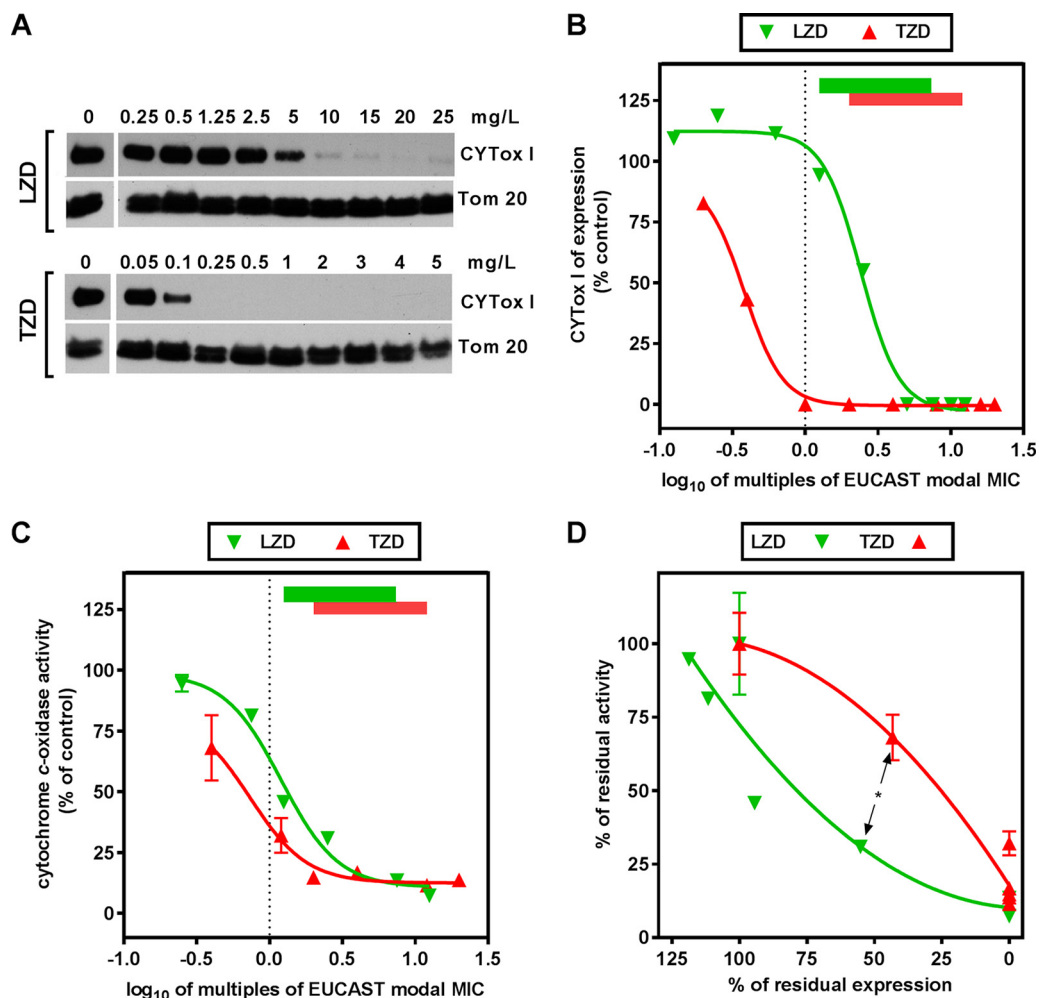


FIG 1 Influence of increasing concentrations of linezolid (LZD) and tedizolid (TZD) on CYTox I expression and cytochrome *c*-oxidase activity in HL-60 promyelocytes incubated for 120 h in the presence of increasing concentrations of these drugs. (A) Western blots of CYTox I and of Tom 20 (used for normalization) of mitochondrial protein fractions. (B) Quantitative measurements of band density ratios (CYTox I to Tom 20) expressed as a percentage of the control value (no oxazolidinone added) and plotted against the oxazolidinone concentrations expressed as \log_{10} of multiples of their respective modal MICs in the EUCAST database (34) (LZD, 2 mg/liter; TZD, 0.25 mg/liter; vertical thin dotted line). Data were used to fit Hill functions (Hill slopes [shared], -3.307 ; $R^2 = 0.99$ [both]) and IC_{50} values (calculated from the Hill functions) for LZD ($2.41 \times$ the MIC or 4.81 mg/liter or $14.2 \mu\text{M}$) or for TZD ($0.383 \times$ the MIC or 0.096 mg/liter or $0.26 \mu\text{M}$). The colored rectangles at the top of the graph refer to typical C_{\min} to C_{\max} ranges of total serum concentrations commonly observed at equilibrium in adult humans receiving currently approved doses of either drug (LZD [green], 2.5 to 15 mg/liter [28]; TZD [red], 0.5 to 3 mg/liter [29, 35]). (C) Activity of cytochrome *c*-oxidase activity in cell lysates normalized to protein content. Data are means \pm the standard deviations (SD) of triplicate determinations in a single, typical experiment (when not visible, SD bars are smaller than the symbols) compared to control values (no oxazolidinone added). The abscissa is in the same units as in panel B. Data were used to fit Hill functions (Hill slopes [shared], -2.224 ; $R^2 = 0.98$ [LZD] and 0.92 [TZD]) and IC_{50} values (calculated from the Hill functions) for LZD ($1.20 \times$ the MIC or 2.41 mg/liter or $7.13 \mu\text{M}$) or for TZD ($0.74 \times$ the MIC or 0.183 mg/liter or $0.49 \mu\text{M}$). The colored rectangles on the top of the graph indicate the C_{\min} -to- C_{\max} ranges of LZD and TZD as in panel B. (D) Correlation between the change in cytochrome *c*-oxidase activity and the impairment of CYTox I expression in experiments illustrated in panels B and C. The data were used to fit second order (quadratic) polynomial functions as this provided the best fit ($R^2 = 0.98$ [LZD] and 0.93 [TZD]; Pearson's $r = 0.909$ [LZD] and 0.968 [TZD]). Based on statistical analysis, the midpoint values (arrows) were significantly different from each other ($P = 0.04$ [two-tailed unpaired *t* test with Welch's correction]). The double arrow points to a statistically difference ($P < 0.05$) in the ratio cytochrome *c*-oxidase activity to CYTox I expression observed at the middle value of CYTox I expression (unpaired *t* test two-tailed test).

almost complete inhibition of CYTox I expression after 48 to 72 h in HL-60 cells. In THP-1 cells, CYTox I expression decreased slower in cells incubated with linezolid than with tedizolid, a complete inhibition being observed after 120 h versus 72 h, respectively. In contrast, the expression of SDHA (one of the four subunits of succinate dehydrogenase complex encoded by nuclear DNA) was not decreased in all these conditions (illustrated for HL-60 cells in Fig. S2 in the supplemental material). Chloramphenicol, used as a

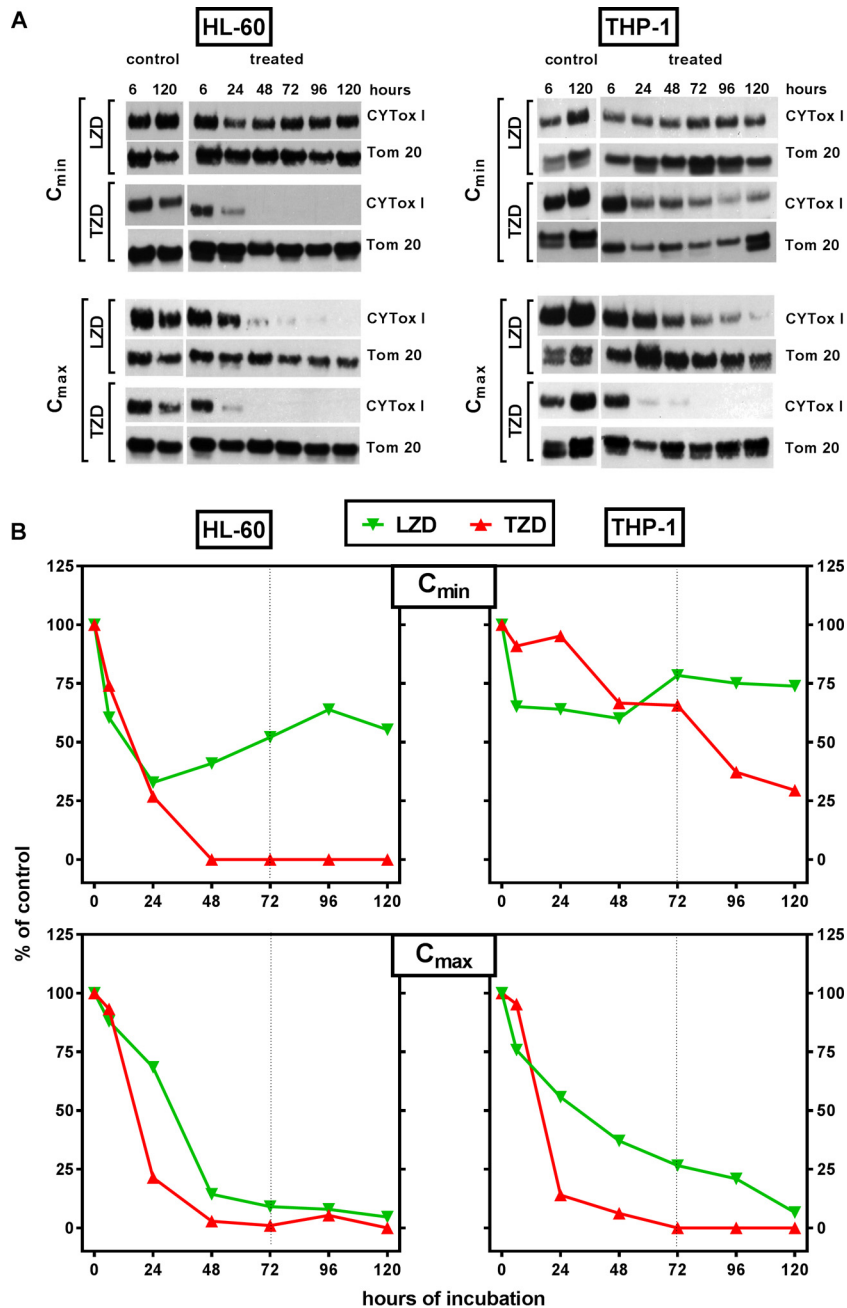


FIG 2 Influence of increasing time of incubation with linezolid (LZD) or tedizolid (TZD) on CYTox I expression in HL-60 promyelocytes and THP-1 monocytes. (A) Western blots of CYTox I and of Tom 20 (used for normalization) of mitochondrial protein fractions, with controls (vehicle only) on the left and increasing times of incubation at two concentrations (C_{min} and C_{max}) corresponding to their total maximal and trough concentrations in humans (LZD, 2.5 and 15 mg/liter [28]; TZD, 0.5 and 3 mg/liter [29, 35]). (B) Quantitative measurements (band density) of the CYTox I/Tom 20 ratio (the vertical dotted line at 72 h refers to the time of incubation selected in further experiments).

positive control, induced complete inhibition of CYTox I expression within 48 h at a concentration of 32 mg/liter (data not shown).

Changes of cytochrome c-oxidase activity and mitochondrial oxygen consumption of HL-60 promyelocytes and THP-1 monocytes after 72 h of incubation at C_{min} and C_{max} . In these experiments, HL-60 and THP-1 cells were maintained for 72 h in the presence of linezolid or tedizolid at C_{min} and C_{max} , since these concentrations had proven to cause intermediate inhibitory effects at C_{min} and maximal inhibitory effects

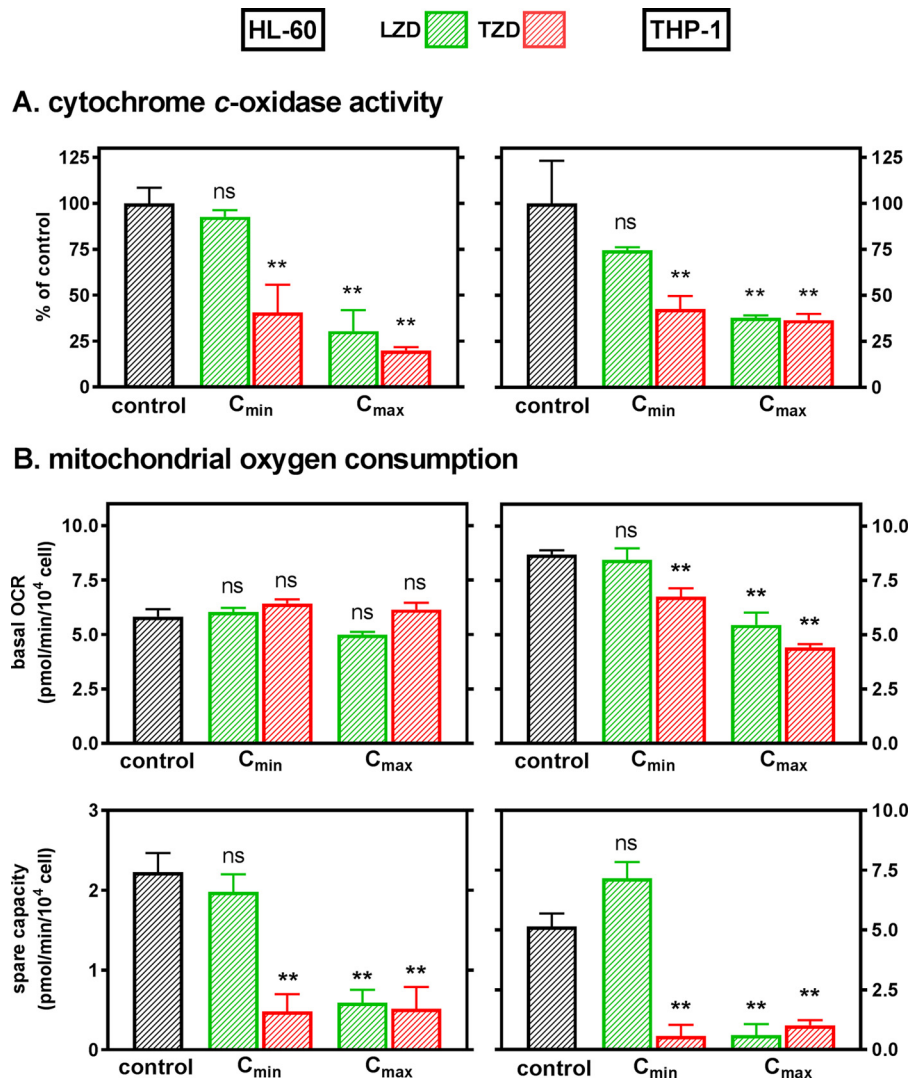


FIG 3 Changes in cytochrome *c*-oxidase activity (A) and mitochondrial respiration (B) (basal oxygen consumption rate [OCR] and spare capacity; see reference 36 and Fig. S3 and Table S1 in the supplemental material for definitions and a full description) in HL-60 promyelocytes (left) and THP-1 monocytes (right) incubated for 72 h in control conditions (white hatched bars) or in the presence of linezolid (LZD) (green hatched bars) or tedizolid (TZD) (red hatched bars) at total extracellular concentrations corresponding to their C_{min} and C_{max} (LZD, 2.5 and 15 mg/liter [28]; TZD, 0.5 and 3 mg/liter [29, 35], respectively). Values are shown as the percent control ± the SD of triplicates for cytochrome *c*-oxidase activity and as means of absolute values ± the standard errors of the mean (SEM) of six to eight wells for mitochondrial oxygen consumption. Statistical analysis using one-way analysis of variance (ANOVA) with Dunnett's multiple comparison of each treatment versus control was performed (ns, $P > 0.05$; *, $P < 0.05$; **, $P < 0.01$).

at C_{max} on CYTox I expression. We first measured the cytochrome *c*-oxidase activity (Fig. 3A). In both cell types exposed to drugs at their C_{min}, the cytochrome *c*-oxidase activity was not decreased by linezolid but was reduced to about 40% by tedizolid. At their C_{max}, both drugs proved to be very inhibitory, leaving only about 10 to 30% of residual activity.

We then measured mitochondrial oxygen consumption using the Seahorse XF technology (see Material and Methods, Fig. S3 in the supplemental material, and reference 36). As shown in Fig. 3B, neither linezolid nor tedizolid affected basal oxygen consumption rate (OCR; considered to essentially meet cell ATP basal demand) in HL-60 cells. However, both linezolid (at C_{max} but not at C_{min}) and tedizolid (at both C_{min} and C_{max}) caused a marked decrease in spare capacity (denoting the inability of cells to meet an increased energy demand). Similar results were obtained with THP-1 cells. Of

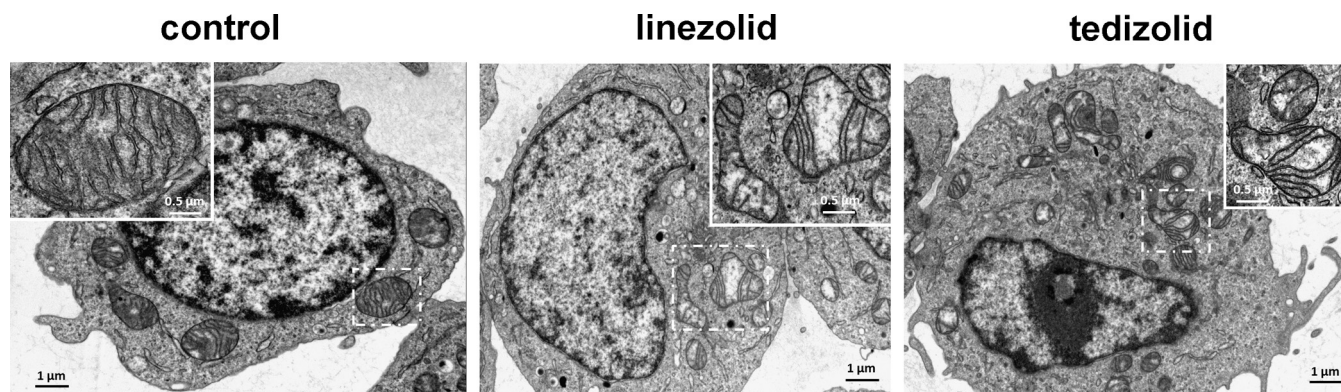


FIG 4 Cell morphology of control and oxazolidinone-treated HL-60 promyelocytes. Representative transmission electron micrographs show cells incubated for 72 h under control conditions or with linezolid or tedizolid at an extracellular concentration corresponding to their human total C_{\max} (linezolid, 15 mg/liter [28]; tedizolid, 3 mg/liter [27, 29]). In each micrograph, one or two representative mitochondria have been selected for inclusion in the corresponding inset to illustrate the distortion of these organelles, the swelling of their matrix, and the loss of cristae in oxazolidinone-treated cells compared to control. Scale bars, 1 μm (0.5 μm in insets).

note, basal OCR and spare capacity were more elevated in THP-1 than in HL-60 cells due to their higher dependence on mitochondrial oxidative metabolism compared to aerobic glycolysis for energy supply (confirmed by observing a lower lactate release/glucose consumption ratio than in HL-60 cells [1.7 ± 0.1] than in THP-1 cells [1.1 ± 0.2] in normoxia).

Effect of oxazolidinones on mitochondrial potential. Mitochondrial potential was measured using tetramethyl rhodamine methyl ester (TMRM [37]). While carbonyl cyanide *m*-chlorophenyl hydrazine (CCCP; an uncoupling agent used as positive control) produced the expected loss of potential, no effect of oxazolidinones was noted at either C_{\min} or C_{\max} (see Fig. S4 in the supplemental material).

Electron microscopy examination of HL-60 promyelocytes and THP-1 monocytes in control conditions and after incubation with linezolid or tedizolid. Figure 4 shows the general morphology of HL-60 cells in control conditions and after incubation with linezolid or tedizolid at C_{\max} during 72 h. Compared to controls, most mitochondria in cells exposed to oxazolidinones showed a decrease in the abundance of inner membrane cristae and a swelling of the matrix (see insets), whereas outer membrane had a normal shape. Other organelles and the general morphology of the cells were otherwise unaffected. Similar observations were made in THP-1 monocytes, but alterations of mitochondrial ultrastructure were less impressive (data not shown).

Uptake of oxazolidinones by HL-60 promyelocytes and THP-1 monocytes. Since linezolid and tedizolid appeared to cause similar levels of mitochondrial toxicity when cells were exposed to concentrations corresponding to their respective C_{\max} values, we measured their total apparent concentration within HL-60 and THP-1 cells incubated for up to 72 h at these concentrations. The results are shown Table 1. Globally, similar cellular apparent concentrations were found for both oxazolidinones at all time points, suggesting that equilibrium had been reached at or before 24 h. It is important to note that the actual tedizolid extracellular concentration (in mg/liter) was 5-fold lower than that of linezolid, indicating that the apparent accumulation of tedizolid was about four times greater on average than that linezolid. In parallel, we followed the efflux of oxazolidinones from HL-60 cells that had been incubated for 72 h with the drugs and then placed in a drug-free medium at 37°C or at 4°C for release. After 30 min, neither oxazolidinone was detectable in cell lysates whatever the temperature (which means that their apparent cellular concentrations were lower than 150 and 300 ng/ml, respectively, of the cell volumes for linezolid and tedizolid).

Reversibility of changes in CYTox I expression, cytochrome *c*-oxidase activity, and mitochondrial respiration in HL-60 promyelocytes. In these experiments, we explored whether the changes seen so far were reversible upon drug withdrawal. To

TABLE 1 Apparent cellular concentrations of linezolid (LZD) or tedizolid (TZD) in HL-60 promyelocytes and THP-1 monocytes^a

Incubation period (h)	Mean apparent cellular concn (mg/liter) \pm SD ^b			
	HL-60		THP-1	
	LZD	TZD	LZD	TZD
24	1.77 \pm 0.45	0.97 \pm 0.15	1.78 \pm 0.08	1.12 \pm 0.12
48	1.48 \pm 0.19*	1.46 \pm 0.37	1.76 \pm 0.60	1.33 \pm 0.25
72	0.83 \pm 0.03	1.25 \pm 0.29	2.95 \pm 0.60	1.50 \pm 0.35

^aThe apparent cellular concentrations of oxazolidinones in HL-60 promyelocytes and THP-1 monocytes were determined upon incubation at extracellular concentrations corresponding to their total human C_{max} (linezolid [LZD], 15 mg/liter [28]; tedizolid [TZD], 3 mg/liter [29, 35]).

^bThe apparent cell content in linezolid or tedizolid was first calculated as ng per mg of total protein sample and then converted to mg per liter of cell volume based on a cell volume/cell total protein ratio of 5 μ l/mg of protein. Values are presented as means \pm the standard deviations ($n = 3$). *, $P < 0.05$ (ANOVA with a Tukey post hoc test comparing values for one drug in one cell type over time).

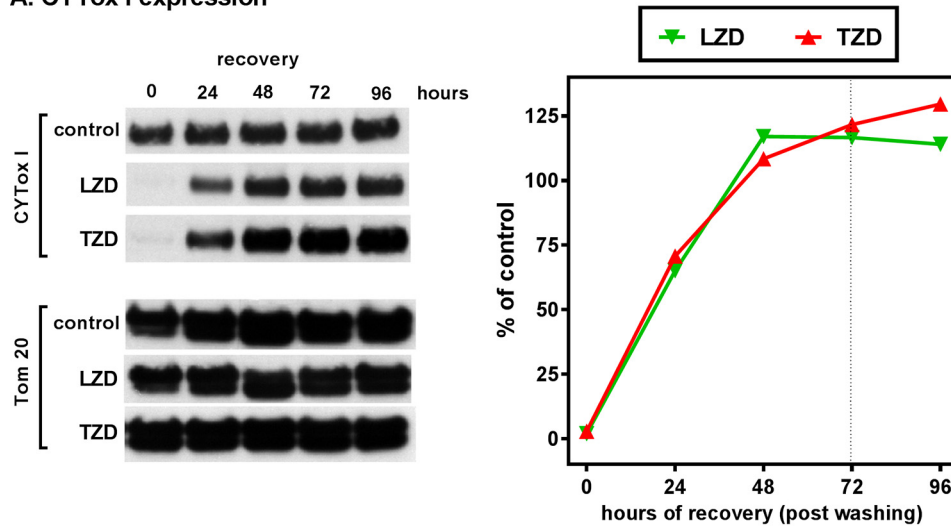
this effect, HL-60 were exposed for 72 h to linezolid or tedizolid at their respective C_{max} values, washed, and reincubated in drug-free medium for up to 96 h. As shown in Fig. 5A, CYTox I expression rose to values slightly above the controls within 48 h after removal of the drug. We then examined the recovery of cytochrome *c*-oxidase activity and of OCR spare capacity in cells that had been incubated for 72 h at C_{min} or C_{max} and then reincubated for 72 h in drug-free medium. The results are shown in Fig. 5B. For cells first incubated with linezolid at C_{min} , and for which no inhibition had been observed, no change over control values was seen. For cells first incubated with linezolid at C_{max} or with tedizolid at either C_{min} or C_{max} , and for which a marked inhibition had been observed (see Fig. 3 and 4), a return to control values was seen for cytochrome *c*-oxidase activity, and a rise to values higher than in controls was noted for OCR spare capacity.

Influence of an intermittent discontinuous exposure to oxazolidinones on CYTox I expression in HL-60 promyelocytes. Based on the latter set of data, we measured CYTox I expression in HL-60 exposed transiently to either linezolid or tedizolid. We took into account differences in schedules of administration and half-lives of linezolid and tedizolid in humans (linezolid, administration BID and $t_{1/2} = 4.3$ to 5.2 h [28]; tedizolid, administration qD and $t_{1/2} = 11$ h [35]). Thus, for linezolid, HL-60 cells were exposed to a concentration corresponding to its C_{max} for 6 h and then transferred to linezolid-free medium for the next 6 h, and the same sequence was repeated up to 96 h (reaching a total of eight exposure/washout sequences). For tedizolid, cells were incubated at a concentration corresponding to its C_{max} for 12 h and then transferred in tedizolid-free medium for the next 12 h, and the same sequence repeated up to 96 h (reaching a total of four exposure/washout sequences). The results are presented in Fig. 6. For linezolid, successive exposures to the drug were without effect for the first 48 h, after which a marked inhibition of CYTox I expression was noted with only partial relief during the washout periods. After 72 h, a semistable level at about 60% of the control value was observed. For tedizolid, an inhibition of CYTox I expression to about 40% of control was observed after the first exposure but was partially relieved during washout. A semistable inhibition at about 50% of control value was observed at 72 h. Residual cell-associated concentration values were measured at the time point corresponding to the trough for each drug and were undetectable.

DISCUSSION

The potential toxicity of oxazolidinones has been recognized early in their preclinical development (23, 24, 38, 39) and its clinical impact for linezolid underlined through an abundance of case reports (see, for example, references 10, 11, 12, 14, 17, 40, 41, 42, and 43), epidemiological studies (see, for example, references 16, 44, 45, 46, 47, and 48), and reviews (7, 49–52), as well as through in-depth *ex vivo* analyses of samples from treated patients (17, 18, 42, 53). Collectively, these studies point to mitochondria as key and selective toxicity targets in eukaryotic cells, with clear evidence of inhibition of the

A. CYTox I expression



B. Cytochrome c-oxidase activity and mitochondrial respiration

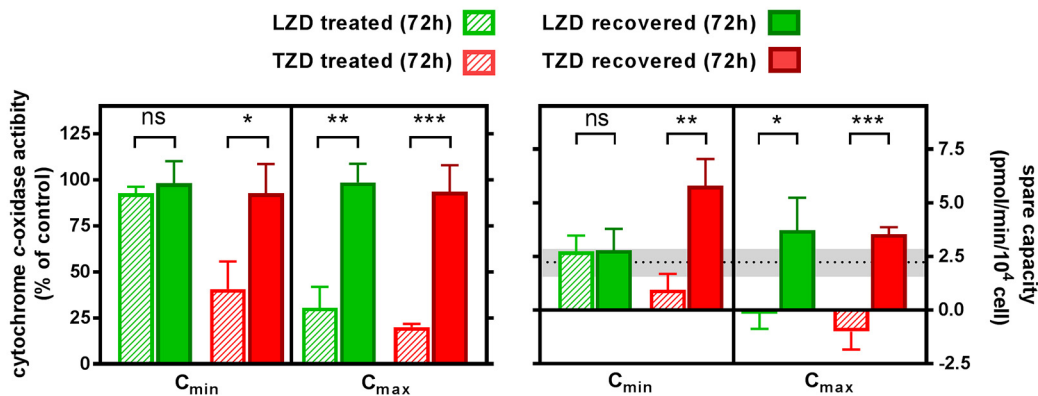


FIG 5 Reversibility of linezolid (LZD)- or tedizolid (TZD)-induced impairment of CYTox I expression (top), cytochrome c-oxidase activity (bottom left), and mitochondrial respiration (spare capacity; bottom right) in HL-60 promyelocytes. (A) Recovery of CYTox I expression over time. Cells were exposed for 72 h to oxazolidinone concentrations corresponding to their total human C_{max} (LZD, 15 mg/liter; TZD, 3 mg/liter) or with vehicle only (control) and thereafter washed and transferred to a drug-free medium for the next 24 to 96 h. The left panel shows Western blot analyses of mitochondrial protein CYTox I and Tom 20 fractions (used for normalization); the right panel presents quantitative measurements (CYTox I/Tom 20 band density ratio). (B) Cytochrome c-oxidase activity and mitochondrial oxygen consumption rate spare capacity 72 h after exposure to oxazolidinone concentrations corresponding to their C_{min} or their C_{max} in humans (treated, hatched bars; LZD, 2.5 or 15 mg/liter; TZD, 0.5 or 3 mg/liter), followed by 72 h of reincubation in drug-free medium (recovery, plain bars). (Left) Cytochrome c-oxidase activity (% of control; means \pm the SD; $n = 3$). (Right) Spare capacity (absolute values; means \pm the SEM of six to eight wells). The thin dotted line shows the mean value observed for control cells, and the gray band indicates the corresponding 95% confidence limits (data from Fig. 4). Statistical analysis was performed using an unpaired t test for a treated versus recovered comparison under each condition (ns, $P > 0.05$; *, $P < 0.05$; **, $P < 0.01$, ***, $P < 0.001$).

synthesis of proteins encoded by the mitochondrial genome being a first and probably causative event in the process leading to main long-term toxicities (see reference 54 for an early review). The present work extends and deepens these observations in several respects for linezolid and adds comparative observations for tedizolid, a newly approved oxazolidinone.

First, throughout the study, we systematically used (or referred to) microbiologically and therapeutically pertinent concentrations (multiples of modal MICs toward *Staphylococcus aureus* [34]; human total peak [C_{max}] and trough [C_{min}] concentrations [28, 29]) to facilitate translation of *in vitro* observations to what may take place in the clinics. In this context, we observed (i) that both drugs selectively inhibit the expression of CYTox I, a protein encoded by the mitochondrial genome, but not SDHA encoded by the nuclear genome, and the activity of cytochrome c-oxidase, a key part of the

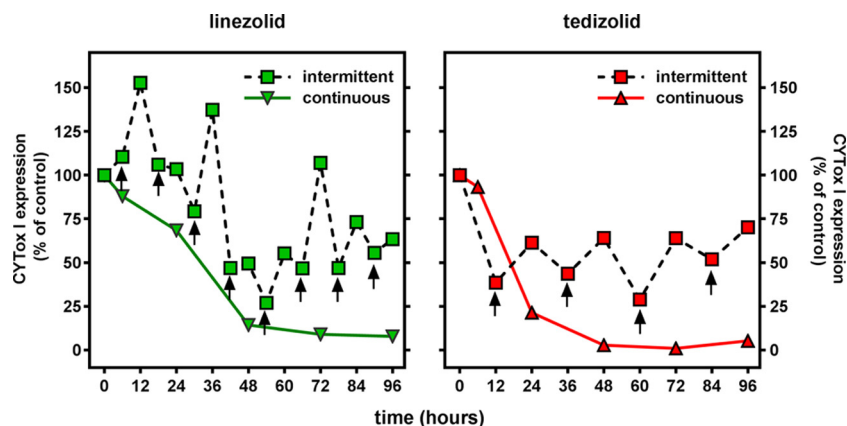


FIG 6 Influence of a discontinuous exposure of HL-60 promyelocytes to linezolid (left) or tedizolid (right), taking into account their differences in approved schedules of administration and half-lives (28, 29, 35) on CYTox I expression. Cells were first exposed to a drug concentration corresponding to its total human C_{max} (linezolid, 15 mg/liter; tedizolid, 3 mg/liter) for 6 h (linezolid) or 12 h (tedizolid), and a sample was taken for assay (indicated by a vertical arrow); the cells were then transferred to drug-free medium for the next 6 h (linezolid) or 12 h (tedizolid), and a new sample was taken. The same sequence was then reproduced for up to 96 h. The ordinate shows the expression level of CYTox I (band density in Western blot [normalized to Tom 20, as in Fig. 2]) as a percentage of the corresponding control [vehicle only]. For comparison, the graphs also show the change in the level of CYTox I expression upon continuous exposure to C_{max} of the same drugs (data from Fig. 2).

mitochondrial electron chain transport; (ii) that these inhibitions are associated with the inability of mitochondria to increase their metabolic oxidative activity upon demand (spare capacity); and (iii) that these effects are fully and quickly reversible upon drug withdrawal. Globally, tedizolid-induced alterations developed at lower concentrations than for linezolid when cells were incubated continuously with the drugs, even when comparisons were made at the same multiples of their modal MICs toward *S. aureus*. This higher toxic potency of tedizolid cannot be ascribed to its higher apparent cellular accumulation, since, at equivalent multiples of their MIC, the two drugs reach similar cell-associated concentrations. In this respect, it is worth mentioning that we cannot exclude that part of these drugs is not truly intracellular but rather associated with the cell surface, since their efflux is rapid at both 37 and 4°C. Additional studies are also needed to determine whether expression of efflux transporters at the cell surface or whether infection would modulate oxazolidinone apparent accumulation within these cells.

Inhibition of CYTox I expression and of complex IV activity upon exposure of cultured cells to oxazolidinones is not a novel observation (see, for example, references 19 and 22). It was also observed in samples from linezolid-treated patients (17, 18). We show here that the inhibition of both CYTox I expression and cytochrome *c*-oxidase activity in cultured cells occurs rapidly upon continuous exposure to oxazolidinones (reaching almost maximal effects in 3 days). Of note, observed IC_{50} values for CYTox I expression compare well with those reported for global mitochondrial protein synthesis as measured *in vitro* (about 9 to 14 μ M for linezolid [19, 22, 55] and about 0.3 μ M for tedizolid [27]). The lower IC_{50} of tedizolid for inhibition of CYTox I expression in comparison with those of linezolid, however, did not translate into more potent inhibition of cytochrome *c*-oxidase activity when the two drugs were compared at microbiologically equipotent concentrations (same multiples of MIC). This is in contrast with early studies comparing oxazolidinones with different antimicrobial potencies (22) and may denote a specific property of tedizolid. Further molecular studies are needed to unravel the mechanisms explaining this divergence. Additional studies should also be performed to understand how cells still maintain about 10 to 15% of cytochrome *c*-oxidase activity under conditions in which CYTox I expression is no more detectable in Western blot analysis.

Second, we showed that both linezolid and tedizolid cause a marked reduction of

mitochondrial spare respiratory capacity (also called reserve capacity), which quantifies how cells respond to an increased ATP demand and withstand periods of stress (36). Changes in this parameter are indicative of major mitochondrial dysfunctions (56, 57) that may not be apparent under basal conditions but will become manifest when ATP demand increases. In this context, unchanged basal OCR evidenced in our study probably results from the maintenance of a low but significant activity of cytochrome *c*-oxidase activity that may be sufficient to meet endogenous energy demand. However, the loss of spare capacity would indicate how close to their bioenergetic limits cells are operating (36). It also heralds a loss of maximal respiration capacity usually associated with a decrease in cristae density, as we report here (see the electron microscopy studies) and was also observed in muscle biopsy specimens of a patient after prolonged use of linezolid (17).

Studies with neuronal cultured cells showed that respiratory spare capacity is essential for cell protection (58) and that its loss enhances susceptibility to stochastic mitochondrial depolarization, leading to major cell energy loss (59). If this concept applies to HL-60 and THP-1 cells, it would explain why no mitochondrial depolarization was observed, because only a limited number of cells would be affected at any time point, making the global assay used here grossly insensitive. However, successive occurrence of stochastic effects *in vivo* may also explain why mitochondrial toxic effects of oxazolidinones eventually translate into overt organ toxicity (such as myelosuppressive effects) only after prolonged treatment times and why they may remain rare (such as neurotoxic effects, for which genetic predisposition may play a critical role [18, 53]).

In a context of screening for drug safety, the combination of cytotoxicity testing using a conventional 3-(4,5-dimethyl-2-thiazolyl)-2,5-diphenyl-2*H*-tetrazolium bromide (MTT) assay (60) made more specific of mitochondrial dysfunction by substituting galactose to glucose as hydrocarbon energy source (61) and of measurements of changes of mitochondrial spare capacity has been shown to be an accurate and sensitive approach for assessing the potential of *in vivo* mitochondrial toxicity of various molecules (62). Using an improved global metabolic assay (MTS), we showed that mitochondrial dysfunction and inhibition of CYTox I expression develop before cytotoxicity. This seems to be in contrast with the approach proposed for drug screening mentioned above, but these studies were more focused on mitochondrial dysfunction and included large, supratherapeutic concentrations of drugs. This may conceal what is probably a concentration-dependent progression in toxic effects from mitochondrial dysfunction to proliferation impairment and then to global cytotoxicity. With respect to proliferation impairment, eperezolid was shown to cause antiproliferative effects at almost the same concentrations at which it caused inhibition of mitochondrial protein synthesis (IC_{50} s of 12 and 9.5 μ M, respectively [19]), whereas we found a much greater divergence between these values (30.8- and 13.8-fold for linezolid and tedizolid, respectively). Actually, the antiproliferative effect of eperezolid was much variable among cell lines (with an IC_{50} up to 63 μ M for HEK cells [19]), suggesting that it could be a late consequence of inhibition of mitochondrial respiration, becoming significant only after critical thresholds specific to cell types and drugs are reached. Some cultured cell lines may also be less susceptible to proliferation inhibition and to cytotoxicity related to mitochondrial dysfunction because they rely more on glycolysis than on mitochondrial metabolism for energy supply.

Third, we found that HL-60 cells were more sensitive to the inhibitory effects of oxazolidinones on protein synthesis than THP-1 cells, while THP-1 cells were slightly more sensitive to their effects on mitochondrial spare capacity. The apparent accumulation of oxazolidinones being similar in both cell types, these differences should therefore rather reflect their specific metabolic characteristics. HL-60 are less differentiated than THP-1 cells and could therefore better represent blood cells progenitors that are a possible target for oxazolidinone-induced anemia or pancytopenia (52). On the other hand, THP-1 cells show a more oxidative metabolism, explaining why their respiratory spare capacity is more affected.

Fourth, we show here that all effects exerted by linezolid and tedizolid on mito-

chondrial protein synthesis, enzyme activity, and mitochondrial respiration are fully reversible. Reversibility of the changes observed in cultured cells exposed to linezolid is not a novel observation (19) and was also noted in peripheral blood mononuclear cells of linezolid-treated patients upon drug discontinuation (18). Interestingly enough, we document here that recovery occurs upon drug withdrawal at the same rate at which inhibition developed during exposure. This is consistent with a noncovalent binding of oxazolidinones to their target sites both in mitochondrial and in bacterial ribosomes, explaining its rapid efflux. Moreover, affinity of oxazolidinones to resting ribosomes *in vitro* is low (with affinity constants of around 90 to 200 μM [63]), which explains why cross-linking approaches using translation-active ribosomes were needed to map their exact site of activity (21, 64). High-affinity binding, responsible for antimicrobial activity, is only transiently and reversibly occurring during the initiation phase of the translation process (64). Low affinity to resting mitochondrial ribosomes would also explain why no stable association of tedizolid with mitochondria could be found by fractionation of cells incubated for short periods of time with this drug in spite of its higher accumulation in cells compared to linezolid (27).

Fifth, throughout the present and previous studies (27), we observed that tedizolid is an as potent or even more potent inhibitor of mitochondrial protein synthesis and of oxidative metabolism than linezolid when comparing drugs at equipotent (multiples of modal MIC) and clinically pertinent (C_{max} and C_{min}) concentrations. This observation was expected since tedizolid shows lower MICs than linezolid toward susceptible bacteria due to the presence of additional target site interactions at the level of the bacterial ribosomes (25), and, therefore, presumably also for the mitochondrial ribosomes. It is also in line with the suggestion that the selection of tedizolid as clinical candidate was based more on improved intrinsic activity (including against linezolid-resistant strains) than safety considerations (24). In phase I studies (with escalating dose and treatment duration up to 21 days), tedizolid was, however, shown to cause less thrombocytopenia (65) and no clinical or subclinical neurologic or ophthalmologic changes (66). Moreover, tedizolid, administered for 9 months to rats at doses up to 8-fold larger than its approved human use did not cause significant neuropathies, which are known to develop with linezolid under these conditions (27). Although remaining limited in terms of dosage and treatment duration, clinical experience of tedizolid safety compares favorably with that of linezolid (67). Interestingly enough, a recent case report suggests that tedizolid could be a useful alternative to linezolid for long-term treatments in cases of inadequate clinical tolerance, myelotoxicity or renal failure (68). The explanation for this better-than-anticipated clinical safety profile may actually stem from the fact that mitochondrial alterations caused by oxazolidinones are reversible. Since tedizolid is administered on a once-daily schedule, it would allow for more prolonged recovery periods (see discussion in reference 27) that could mitigate its higher intrinsic toxicity compared to linezolid. Further clinical experience with longer treatment durations than currently approved are, however, needed to assess the true safety potential of tedizolid.

The present study has clear limitations. First, all comparisons were made in media with low protein content (10% serum), which minimizes drug protein binding and tends to equate free and total concentrations of linezolid and tedizolid. This could not be avoided since it is impossible to grow and maintain cells in media containing substantially larger proportions of serum. However, we know that tedizolid is 70 to 90% protein-bound in human plasma (29) versus 31% for linezolid (28). If only the free fractions of oxazolidinones must be considered, then comparisons in our cell culture model would need to be made with lower C_{min} and C_{max} values for tedizolid than those used here, which would make it to appear less inhibitory than what we present. It could also be part of the explanation as to why safety clinical data for tedizolid are more favorable than anticipated based on *in vitro* studies. A second limitation, with respect to the development of clinically meaningful mid- and long-term toxicities, is that all experiments were made with short-term exposures. Thus, for instance, myelosuppressive effects of oxazolidinones may involve a succession of events originating in early

interactions of the drugs with progenitor cells but for which clinical expression becomes only visible at the end of the differentiation/maturation process (see reference 69 for a modeling of the succession of toxic events in a pharmacokinetic-toxicodynamic context). This could be addressed in further studies, pending the development of appropriate *in vitro* tools.

MATERIALS AND METHODS

Drugs and cells. Tedizolid (TZD) was obtained as a microbiological standard first from Trius Pharmaceuticals (San Diego, CA) and thereafter from Cubist Pharmaceuticals GmbH (Zürich, Switzerland), now both parts of Merck & Co. (Kenilworth, NJ). Linezolid (LZD) was obtained as RX-0366-00-005 (product for *in vitro* investigations) from RibX Pharmaceuticals (presently Melinta Therapeutics, New Haven, CT). Chloramphenicol was obtained from Sigma-Aldrich (St. Louis, MO). Stock solutions were prepared in dimethyl sulfoxide (DMSO) and thereafter diluted in the appropriate medium to reach the desired concentration, with the DMSO final concentration in the culture fluid adjusted to 0.5% (allowing us to take into consideration a possible effect of DMSO on cell differentiation). The stability of the drugs at their free human C_{max} was checked during 72 h of incubation in RPMI 1640 complemented or not by fetal bovine serum and in phosphate-buffered saline (PBS) using the high-pressure liquid chromatography (HPLC) assay described below. No degradation was evidenced. The human promyelocytic leukemia cells HL-60 (30, 31) and the human monocytes THP-1 (32) were obtained from the American Tissue Culture Collection (Manassas, VA) and grown in RPMI 1640 medium containing 2 g/liter glucose and 0.3 g/liter glutamine and supplemented with 10% fetal bovine serum (Gibco-Life Technologies/Thermo-Fisher Scientific, Inc., Waltham, MA). Cells were maintained at a density between 10^5 and 5×10^5 cells/ml and incubated at 37°C in a 5% CO₂-air atmosphere. Their proliferation was evaluated by cell counting using an automated cell counter (Beckman Coulter Life Science, Indianapolis, IN).

Preparation of a fraction enriched in mitochondria. We followed a published procedure (19) with minor modifications. In brief, cells were seeded at 2×10^5 to 3×10^5 cells/ml in 75-cm² flasks, in a total volume of 50 ml for different incubation periods and then collected, washed once with PBS, resuspended in 1 ml of TKM buffer (10 mM Tris-HCl [pH 7.5], 10 mM KCl, 0.15 mM NaCl) and homogenized with 40 strokes of the tight pestle (pestle B) of a Dounce tissue grinder (Thomas Scientific, Swedesboro, NJ). The absence of intact cells in homogenates was checked by microscopic examination. A 300- μ l portion of TKM buffer containing 1 M sucrose was added, and the samples were centrifuged at $1,000 \times g$ for 5 min. Supernatants were collected and centrifuged at $5,000 \times g$ for 20 min. Pellets were resuspended in a suitable volume (usually 70 to 100 μ l) of TKM buffer containing 0.25 M sucrose. The protein content of the fraction was determined using a bicinchoninic acid assay (BCA protein assay reagent; Pierce/Thermo Fisher, Waltham, MA).

Western blot analysis. Mitochondrial fractions were electrophoresed on precasted NuPAGE 10% Bis-Tris gels (Novex; Life Technologies/Thermo Fisher) and wet transferred to polyvinylidene fluoride membranes (Thermo Fisher), which were blocked for 1 h at room temperature with 5% dry milk in Tris-buffered saline containing 0.05% Tween 20. Membranes were then incubated overnight at 4°C (or for 1 h at room temperature) with 1 μ g/ml mouse anti-cytochrome *c*-oxidase subunit I (CYTox I) monoclonal antibody (Anti-OxPhos Complex IV subunit I monoclonal antibody; Invitrogen, catalog no. 459600 [Thermo Fisher]) or with 0.1 μ g/ml mouse anti-succinate dehydrogenase monoclonal antibody (Anti-Complex II 70-kDa Fp subunit monoclonal antibody; Invitrogen, catalog no. 459200 [Thermo Fisher]) and then with an appropriate secondary antibody (0.08 μ g/ml) coupled to horseradish peroxidase (Santa Cruz Biotechnology, Inc., Santa Cruz, CA) for 1 h at room temperature. Blots were revealed using the SuperSignal West Pico chemiluminescent substrate (Thermo Fisher) and a Fuji Film FPM-100A apparatus (Fuji Films, Minato-ku, Tokyo) and CL-XPosure films (Thermo Fisher). Stripped membranes (30 min incubation at room temperature or 4°C in Restore Western blot stripping buffer; Thermo Fisher) were then incubated 1 h at room temperature with 0.02 μ g/ml of rabbit anti-Tom 20 polyclonal antibody (Santa Cruz Biotechnology, catalog no. FL-145) and then with an anti-rabbit IgG antibody coupled to horseradish peroxidase (Santa Cruz Biotechnology) to allow for chemiluminescence detection. The band intensity was quantified on scanned films (GelDoc; Bio-Rad, Hercules, CA) using ImageJ software (National Institutes of Health, Bethesda, MD [<https://imagej.nih.gov/ij/>]).

Cytochrome *c*-oxidase activity. Cells were seeded at 1×10^5 to 2×10^5 cells/ml in six-well plates, in a total volume of 6 ml for different periods of time and then pelleted by low-speed centrifugation, washed three times in PBS at 4°C, and resuspended in ice-cold water. Suspensions were sonicated (two to three times for 10 s at a maximum of 100 W; B. Braun Labsonic L; Braun Biotech International, Melsungen, Germany) and mixed with an equal volume of 0.4% digitonin. The cytochrome *c*-oxidase activity was assayed as previously described (70). Briefly, a 540-mg/liter solution of cytochrome *c* (from bovine heart; Sigma-Aldrich, catalog no. C7752) was carefully added with sodium dithionite to achieve a 90 to 95% reduction (to avoid any excess of reducing agent) and 1.5 ml mixed with 50 μ l of cell lysate. Cytochrome *c* oxidation was followed by the decrease in its absorbance at 550 nm over 10 min (Genesys 2 spectrophotometer; Thermo Spectronic, Rochester, NY), after which complete oxidation was achieved by addition of K₃Fe(CN)₆ in order to measure the background absorbance value of the samples. Cytochrome *c*-oxidase activity was calculated as the slope of the change in absorbance over time after logarithmic linearization. Data were normalized by the protein content of the cell lysate, determined by Lowry's method (71).

Cytotoxicity assay (MTS assay). We used a CellTiter 96 Aqueous nonradioactive cell proliferation assay (Promega, Madison, WI) with 3-(4,5-dimethylthiazol-2-yl)-5-(3-carboxymethoxyphenyl)-2-(4-

sulfophenyl)-2H-tetrazolium inner salt (MTS) being reduced into a colored formazan product soluble in tissue culture medium. This conversion, which is accomplished by NADPH or NADH produced by cell dehydrogenases (72), is an index of the number of metabolically active cells (73). Cells (cultured as described in the previous paragraph) were directly incubated with MTS tetrazolium salt for 1 h at 37°C, and the absorbance was read at 490 nm.

Mitochondrial oxygen consumption rate measurements. Cells were seeded at 1×10^5 to 2×10^5 cells/ml in 25-cm² flasks in a total volume of 9 ml for 72 h and then counted, collected by low-speed centrifugation, resuspended at a suitable dilution in unbuffered Dulbecco modified Eagle medium (catalog no. D5030; Sigma-Aldrich) supplemented with 1.85 g/liter NaCl, 10 mM D-glucose, and 2 mM L-glutamine, and seeded in a poly-L-lysine-coated (poly-L-lysine hydrobromide; Sigma-Aldrich, catalog no. P6282) Seahorse XF96 V3 PS cell culture microplate (catalog no. 101085-004; Agilent Technologies, Santa Clara, CA) at densities of 250,000 and 50,000 cells/well for HL-60 promyelocytes and THP-1 monocytes, respectively. The oxygen consumption rate (OCR) was then measured using an XF Cell Mito stress test kit (Agilent, catalog no. 103015-100) on a Seahorse XF96 analyzer (Seahorse Bioscience, North Billerica, MA) according to the manufacturer's instructions. The following drugs were successively injected (with final concentrations as indicated): oligomycin (1 μ M), 2-[4-(trifluoromethoxy)phenyl]hydrazinylidene]propanedinitrile (FCCP; 2 μ M), and rotenone/antimycin A (0.5 μ M each). The basal mitochondrial OCR was determined as the difference between OCR measured before any injection and OCR measured after injection of rotenone/antimycin A (which corresponds to the nonmitochondrial respiration). Spare capacity was the difference between OCR measured after FCCP injection (maximal respiration) and OCR measured before any injection (see Fig. S3 in the supplemental material for an illustration, supplemental Table S1 for definitions, and references 36 and 74 for general and technical descriptions, respectively). Data were normalized by cell counting using a SpectraMax i3 plate imager (Molecular Devices, Sunnyvale, CA) and SoftMax Pro software (Molecular Devices).

Glucose consumption and lactate release measurements. About 2×10^5 to 3×10^5 cells were seeded in 3 ml of RPMI 1640 medium (containing L-glutamine) and left untreated or treated for 48 h, after which the cells were removed by centrifugation, and the supernatant was deproteinized by high-speed centrifugation ($14,000 \times g$; 20 min; centrifuge model 5417; Eppendorf AG, Hamburg, Germany) through a 10-kDa cutoff polyethersulfone membrane (centrifugal filter tubes, catalog no. 516-0230; VWR International Ltd., Dublin, Ireland). The D-glucose and L-lactate concentrations were then measured in the ultrafiltrate by a colorimetric enzyme-based assay using a CMA-600 analyzer (CMA Microdialysis AB, Kista, Sweden) according to the manufacturer's instructions.

Mitochondrial potential measurement. Membrane potential was assessed using tetramethyl rhodamine methyl ester (TMRM; Sigma-Aldrich), a cell-permeant cationic lipophilic red fluorescent dye that accumulates in mitochondria in function of mitochondrial membrane potential (37). Cells were seeded at 2×10^5 to 3×10^5 cells/ml in 75-cm² flasks in a total volume of 35 ml for 72 h. One million cells were collected by centrifugation ($200 \times g$; 5 min) at room temperature, washed with PBS, resuspended in 1 ml of cell culture medium containing TMRM at a final concentration of 10 nM, and incubated for 30 min at 37°C. Cells were centrifuged again, washed with PBS, and resuspended in 1 ml of PBS containing 2 mM EDTA and 0.5% bovine serum albumin. Fluorescence-activated cell sorting (FACS) analysis for TMRM was performed in FL2 channel on a BD FACSCalibur instrument (BD Bioscience, Franklin Lakes, NJ) with CellQuest software and analyzed using FlowJo software (Tree Star, Inc., Ashland, OR).

Electron microscopy. Cells were seeded at 5×10^5 to 6×10^5 cells/ml in 75-cm² flasks, with a total volume of 50 ml for 72 h. Control and oxazolidinone-treated HL-60 promyelocytes were collected by low-speed centrifugation ($600 \times g$; 10 min), resuspended, and maintained in 2% glutaraldehyde–0.1 M sodium cacodylate buffer (pH 7.4) for 30 min at 4°C. After one rinse in glutaraldehyde-free buffer, the cells were postfixed in 1% osmium tetroxide for 1 h at 4°C, rinsed once in cacodylate buffer, rinsed once in 0.15 M NaCl, rinsed once in 0.02 M veronal acetate (pH 7), and thereafter stained *en bloc* with 0.5% uranyl acetate for 1 h at room temperature. Samples were then pelleted in melted agar, dehydrated by successive immersion in 70, 90, and 100% ethanol, and embedded using an agar low-viscosity resin kit (R1078; Agar Scientific, Ltd., Stansted, United Kingdom) according to the manufacturer's procedures. Ultrathin sections (70 nm) were stained with lead citrate and uranyl acetate and observed in a Philips CM-12 transmission electron microscope (Philips, Amsterdam, The Netherlands) operated at 80 kV.

Measurement of apparent cellular oxazolidinone concentrations. Cells were seeded at 6×10^5 to 7×10^5 cells/ml in 75-cm² flasks, with a total volume of 35 ml and exposed to linezolid or tedizolid for up to 72 h, collected by low-speed centrifugation ($600 \times g$, 10 min), subjected to three successive washes in ice-cold PBS, resuspended in distilled water (75), and mixed with an internal standard ([²H₃]linezolid at 1 mg/liter or [¹³C,²H₃]tedizolid at 1.5 mg/liter, both from Alsachim SAS, Illkirch, France). When measuring efflux, cells incubated for appropriated times with the drugs were washed as described above and replaced in fresh, drug-free medium for appropriate times, washed again, and mixed with internal standard. Samples were then sonicated (two to three times 10 s at a maximum of 100 W [B. Bran Labsonic L]), and the resulting lysates were used for the determination of the oxazolidinone concentration by HPLC-MS with a LTQ-Orbitrap mass spectrometer (Thermo Fisher Scientific) coupled to an Accela HPLC system (Thermo Fisher Scientific). Portions (100 μ l) of cell lysate were deproteinized with 750 μ l of acetonitrile-methanol (21:4), vortexed, frozen at -20°C for 30 min, thawed, and centrifuged at $11,000 \times g$ for 5 min. The supernatant was evaporated under an air stream, the residue was reconstituted in 100 μ l of methanol, and 25 μ l was injected into the HPLC system. Analyte separation was achieved using a C-18 Supelco precolumn and a Supelcosil C-18 column (3 μ m, 4 by 150 mm; Supelco). Mobile phases A and B were composed of methanol-H₂O (75:25 [vol/vol]) and methanol, respectively, both supplemented with 0.1% of acetic acid. The gradient (0.4 ml/min) was designed as follows: transition from 100% A to

100% B in 20 min, followed by 100% B linearly over 10 min, and followed by a subsequent reequilibration at 100% A. Analytes were ionized using an electrospray ionization source operated in positive mode (spray voltage set at 5.0 kV; capillary temperature, 270°C; sheath gas flow, 40 arbitrary units). The signals were normalized using the value obtained for the corresponding internal standard. The assay was linear for concentrations ranging from 0.05 to 2.4 mg/liter for linezolid and 0.025 to 3.2 mg/liter for tedizolid. The accuracy of the method expressed as bias (in %) was determined for both linezolid and tedizolid at four concentration levels ranging from 0.1 to 1 mg/liter. The bias for the intraday accuracy were comprised between -1.37 and 1.45% (linezolid) and between 3.84 and 2.50% (tedizolid); those for interday accuracy were comprised between 0.80 and 0.76% (linezolid) and between 1.39 and 2.13% (tedizolid). The repeatability (expressed as the %CV of the data obtained on three measurements on three different days) ranged between 2.72 and 2.97% (linezolid) and between 1.04 and 3.94% (tedizolid). These values were below the limit of acceptance of 15% as recommended by the international guidelines. The limits of detection were 50 ng/ml (linezolid) and 25 ng/ml (tedizolid). Apparent cellular concentrations of oxazolidinones were calculated using a cell volume to protein ratio of 5 μ l/mg protein as determined experimentally in cultured cells (76) and used in our previous studies with tedizolid and THP-1 monocytes (75).

Statistical analyses. Curve fitting and statistical analyses were performed using GraphPad Prism version 7.3 and GraphPad InStat version 3.10 both for Windows (GraphPad Software, Inc., San Diego, CA).

Source of products. Products not described above were obtained from Sigma-Aldrich or Merck KGaA (Darmstadt, Germany).

SUPPLEMENTAL MATERIAL

Supplemental material for this article may be found at <https://doi.org/10.1128/AAC.01599-17>.

SUPPLEMENTAL FILE 1, PDF file, 0.5 MB.

ACKNOWLEDGMENTS

M. C. Cambier, V. Mohymont, P. Muller, and K. Santos Saial provided skillful technical assistance. We thank E. André (Pôle de Pharmacologie et Thérapeutique, Institut de Recherche Expérimentale et Clinique, Université catholique de Louvain) for help in the determination of mitochondrial potential, S. Constantinescu (Cell Signaling, De Duve Institute, Université catholique de Louvain) for access to automated cell counter, and the MASSMET platform (<https://uclouvain.be/en/research-institutes/ldri/massmet.html>) for access to high-pressure liquid chromatography mass spectrometry.

This study received no specific grant from any funding agency in the public, commercial, or not-for-profit sectors and was covered by the general budget of the participating laboratories. T.V.M. and G.G.M. are employees of the Université catholique de Louvain, V.L.P. is a Research Fellow, P.S. is a Senior Research Associate, and F.V.B. is a Research Director of the FRS-FNRS. P.M.T. is an unpaid emeritus professor and has received speaker's honoraria from Bayer and research grants from Trius for works different from what is being submitted here. The other authors have nothing to declare.

REFERENCES

- Swaney SM, Aoki H, Ganoza MC, Shinabarger DL. 1998. The oxazolidinone linezolid inhibits initiation of protein synthesis in bacteria. *Antimicrob Agents Chemother* 42:3251–3255.
- Wilson DN, Schluenzen F, Harms JM, Starosta AL, Connell SR, Fucini P. 2008. The oxazolidinone antibiotics perturb the ribosomal peptidyl-transferase center and effect tRNA positioning. *Proc Natl Acad Sci U S A* 105:13339–13344. <https://doi.org/10.1073/pnas.0804276105>.
- Livermore DM. 2003. Linezolid *in vitro*: mechanism and antibacterial spectrum. *J Antimicrob Chemother* 51(Suppl 2):ii9–ii16. <https://doi.org/10.1093/jac/dkg249>.
- Kristich CJ, Rice LB, Arias CA. 2014. Enterococcal infection: treatment and antibiotic resistance, p 123–184. *In* Gilmore MS, Clewell DB, Ike Y, Shankar N (ed), *Enterococci: from commensals to leading causes of drug-resistant infection*. Massachusetts Eye and Ear Infirmary, Boston, MA.
- Bassetti M, Baguneid M, Bouza E, Dryden M, Nathwani D, Wilcox M. 2014. European perspective and update on the management of complicated skin and soft tissue infections due to methicillin-resistant *Staphylococcus aureus* after more than 10 years of experience with linezolid. *Clin Microbiol Infect* 20(Suppl 4):3–18. <https://doi.org/10.1111/1469-0691.12463>.
- Aksoy DY, Unal S. 2008. New antimicrobial agents for the treatment of Gram-positive bacterial infections. *Clin Microbiol Infect* 14:411–420. <https://doi.org/10.1111/j.1469-0691.2007.01933.x>.
- Moellering RC. 2003. Linezolid: the first oxazolidinone antimicrobial. *Ann Intern Med* 138:135–142. <https://doi.org/10.7326/0003-4819-138-2-200301210-00015>.
- Cox HL, Donowitz GR. 2015. Chapter 32. Linezolid and other oxazolidinones. *In* Bennett JE, Dolin R, Blaser MJ (ed), *Mandell, Douglas, and Bennett's principles and practice of infectious diseases*. Elsevier, New York, NY.
- Gould IM, David MZ, Esposito S, Garau J, Lina G, Mazzei T, Peters G. 2012. New insights into methicillin-resistant *Staphylococcus aureus* (MRSA) pathogenesis, treatment and resistance. *Int J Antimicrob Agents* 39:96–104. <https://doi.org/10.1016/j.ijantimicag.2011.09.028>.
- Gerson SL, Kaplan SL, Bruss JB, Le V, Arellano FM, Hafkin B, Kuter DJ. 2002. Hematologic effects of linezolid: summary of clinical experience. *Antimicrob Agents Chemother* 46:2723–2726. <https://doi.org/10.1128/AAC.46.8.2723-2726.2002>.
- Bernstein WB, Trotta RF, Rector JT, Tjaden JA, Barile AJ. 2003. Mechanisms for linezolid-induced anemia and thrombocytopenia. *Ann Pharmacother* 37:517–520. <https://doi.org/10.1345/aph.1C361>.

12. Apodaca AA, Rakita RM. 2003. Linezolid-induced lactic acidosis. *N Engl J Med* 348:86–87. <https://doi.org/10.1056/NEJM200301023480123>.
13. Santini A, Ronchi A, Garbellini M, Piga D, Protti A. 2017. Linezolid-induced lactic acidosis: the thin line between bacterial and mitochondrial ribosomes. *Expert Opin Drug Saf* 16:833–843.
14. Bressler AM, Zimmer SM, Gilmore JL, Somani J. 2004. Peripheral neuropathy associated with prolonged use of linezolid. *Lancet Infect Dis* 4:528–531. [https://doi.org/10.1016/S1473-3099\(04\)01109-0](https://doi.org/10.1016/S1473-3099(04)01109-0).
15. Darley ESR, MacGowan AP. 2004. Antibiotic treatment of gram-positive bone and joint infections. *J Antimicrob Chemother* 53:928–935. <https://doi.org/10.1093/jac/dkh191>.
16. Pea F, Viale P, Cojutti P, Del Pin B, Zamparini E, Furlanut M. 2012. Therapeutic drug monitoring may improve safety outcomes of long-term treatment with linezolid in adult patients. *J Antimicrob Chemother* 67:2034–2042. <https://doi.org/10.1093/jac/dks153>.
17. De Vriese AS, Coster RV, Smet J, Seneca S, Lovering A, Van Haute LL, Vanopdenbosch LJ, Martin JJ, Groote CC, Vandecasteele S, Boelaert JR. 2006. Linezolid-induced inhibition of mitochondrial protein synthesis. *Clin Infect Dis* 42:1111–1117. <https://doi.org/10.1086/501356>.
18. Garrabou G, Soriano A, Lopez S, Gualar JP, Giral M, Villarroya F, Martinez JA, Casademont J, Cardellach F, Mensa J, Miro O. 2007. Reversible inhibition of mitochondrial protein synthesis during linezolid-related hyperlactatemia. *Antimicrob Agents Chemother* 51:962–967. <https://doi.org/10.1128/AAC.01190-06>.
19. Nagiec EE, Wu L, Swaney SM, Chosay JG, Ross DE, Brieland JK, Leach KL. 2005. Oxazolidinones inhibit cellular proliferation via inhibition of mitochondrial protein synthesis. *Antimicrob Agents Chemother* 49:3896–3902. <https://doi.org/10.1128/AAC.49.9.3896-3902.2005>.
20. Sharma MR, Koc EC, Datta PP, Booth TM, Spremulli LL, Agrawal RK. 2003. Structure of the mammalian mitochondrial ribosome reveals an expanded functional role for its component proteins. *Cell* 115:97–108. [https://doi.org/10.1016/S0092-8674\(03\)00762-1](https://doi.org/10.1016/S0092-8674(03)00762-1).
21. Leach KL, Swaney SM, Colca JR, McDonald WG, Blinn JR, Thomasco LM, Gadwood RC, Shinabarger D, Xiong L, Mankin AS. 2007. The site of action of oxazolidinone antibiotics in living bacteria and in human mitochondria. *Mol Cell* 26:393–402. <https://doi.org/10.1016/j.molcel.2007.04.005>.
22. McKee EE, Ferguson M, Bentley AT, Marks TA. 2006. Inhibition of mammalian mitochondrial protein synthesis by oxazolidinones. *Antimicrob Agents Chemother* 50:2042–2049. <https://doi.org/10.1128/AAC.01411-05>.
23. Shaw KJ, Barbachyn MR. 2011. The oxazolidinones: past, present, and future. *Ann N Y Acad Sci* 1241:48–70. <https://doi.org/10.1111/j.1749-6632.2011.06330.x>.
24. Renslo AR. 2010. Antibacterial oxazolidinones: emerging structure-toxicity relationships. *Expert Rev Anti Infect Ther* 8:565–574. <https://doi.org/10.1586/eri.10.26>.
25. Shaw KJ, Poppe S, Schaadt R, Brown-Driver V, Finn J, Pillar CM, Shinabarger D, Zurenko G. 2008. In vitro activity of TR-700, the antibacterial moiety of the prodrug TR-701, against linezolid-resistant strains. *Antimicrob Agents Chemother* 52:4442–4447. <https://doi.org/10.1128/AAC.00859-08>.
26. Im WB, Choi SH, Park JY, Choi SH, Finn J, Yoon SH. 2011. Discovery of torezolid as a novel 5-hydroxymethyl-oxazolidinone antibacterial agent. *Eur J Med Chem* 46:1027–1039. <https://doi.org/10.1016/j.ejmech.2011.01.014>.
27. Flanagan S, McKee EE, Das D, Tulkens PM, Hosako H, Fiedler-Kelly J, Passarell J, Radovsky A, Prokocimer P. 2015. Nonclinical and pharmacokinetic assessments to evaluate the potential of tedizolid and linezolid to affect mitochondrial function. *Antimicrob Agents Chemother* 59:178–185. <https://doi.org/10.1128/AAC.03684-14>.
28. Anonymous. 2015. Zyvox: linezolid injection solution. Prescribing information. Pharmacia and Upjohn Company, Division of Pfizer, Inc, New York, NY. <http://labeling.pfizer.com/showlabeling.aspx?id=649>.
29. Merck Sharp & Dohme. 2016. Sivextro (tedizolid phosphate) for injection, for intravenous use: prescribing information. Merck Sharp & Dohme Corp., a subsidiary of Merck & Co., Inc, White House Station, NJ. https://www.merck.com/product/usa/pi_circulars/s/sivextro/sivextro_pi.pdf.
30. Collins SJ, Ruscetti FW, Gallagher RE, Gallo RC. 1978. Terminal differentiation of human promyelocytic leukemia cells induced by dimethyl sulfoxide and other polar compounds. *Proc Natl Acad Sci U S A* 75:2458–2462. <https://doi.org/10.1073/pnas.75.5.2458>.
31. Gallagher R, Collins S, Trujillo J, McCredie K, Ahearn M, Tsai S, Metzgar R, Aulakh G, Ting R, Ruscetti F, Gallo R. 1979. Characterization of the continuous, differentiating myeloid cell line (HL-60) from a patient with acute promyelocytic leukemia. *Blood* 54:713–733.
32. Tsuchiya S, Yamabe M, Yamaguchi Y, Kobayashi Y, Konno T, Tada K. 1980. Establishment and characterization of a human acute monocytic leukemia cell line (THP-1). *Int J Cancer* 26:171–176. <https://doi.org/10.1002/ijc.2910260208>.
33. Lemire B. 2005. Mitochondrial genetics, p 1–10. In Hodgkin J, Anderson P (ed), *Wormbook: The Caenorhabditis elegans research community*. <https://doi.org/10.1895/wormbook.1.25.1>.
34. EUCAST. 2017. Antimicrobial wild-type distributions of microorganisms. European Committee on Antimicrobial Susceptibility Testing, Copenhagen, Denmark. <https://mic.eucast.org/Eucast2/>.
35. Flanagan S, Fang E, Munoz KA, Minassian SL, Prokocimer PG. 2014. Single- and multiple-dose pharmacokinetics and absolute bioavailability of tedizolid. *Pharmacotherapy* 34:891–900. <https://doi.org/10.1002/phar.1458>.
36. Divakaruni AS, Paradyse A, Ferrick DA, Murphy AN, Jastroch M. 2014. Analysis and interpretation of microplate-based oxygen consumption and pH data. *Methods Enzymol* 547:309–354. <https://doi.org/10.1016/B978-0-12-801415-8.00016-3>.
37. Rowe I, Chiaravalli M, Mannella V, Ulisse V, Quilici G, Pema M, Song XW, Xu H, Mari S, Qian F, Pei Y, Musco G, Boletta A. 2013. Defective glucose metabolism in polycystic kidney disease identifies a new therapeutic strategy. *Nat Med* 19:488–493. <https://doi.org/10.1038/nm.3092>.
38. Barbachyn MR, Ford CW. 2003. Oxazolidinone structure-activity relationships leading to linezolid. *Angew Chem Int Ed Engl* 42:2010–2023. <https://doi.org/10.1002/anie.200200528>.
39. Brickner SJ, Barbachyn MR, Hutchinson DK, Manninen PR. 2008. Linezolid (ZYVOX), the first member of a completely new class of antibacterial agents for treatment of serious gram-positive infections. *J Med Chem* 51:1981–1990. <https://doi.org/10.1021/jm800038g>.
40. Kopterides P, Papadomichelakis E, Armaganidis A. 2005. Linezolid use associated with lactic acidosis. *Scand J Infect Dis* 37:153–154. <https://doi.org/10.1080/00365540410026022>.
41. Pea F, Scudeller L, Lugano M, Baccarani U, Pavan F, Tavio M, Furlanut M, Rocca GD, Bresadola F, Viale P. 2006. Hyperlactacidemia potentially due to linezolid overexposure in a liver transplant recipient. *Clin Infect Dis* 42:434–435. <https://doi.org/10.1086/499533>.
42. Azamfirei L, Copotoiu SM, Branzaniuc K, Szederjesi J, Copotoiu R, Ber-teanu C. 2007. Complete blindness after optic neuropathy induced by short-term linezolid treatment in a patient suffering from muscle dystrophy. *Pharmacoepidemiol Drug Saf* 16:402–404. <https://doi.org/10.1002/pds.1320>.
43. Poulakos MN, Grace Y, Coakley C. 2012. Probable linezolid-induced thrombocytopenia in a patient with vancomycin-resistant enterococci. *J Pharm Pract* 25:615–618. <https://doi.org/10.1177/0897190012442720>.
44. Hanai Y, Matsuo K, Ogawa M, Higashi A, Kimura I, Hirayama S, Kosugi T, Nishizawa K, Yoshio T. 2016. A retrospective study of the risk factors for linezolid-induced thrombocytopenia and anemia. *J Infect Chemother* 22:536–542. <https://doi.org/10.1016/j.jiac.2016.05.003>.
45. Ichie T, Suzuki D, Yasui K, Takahashi H, Matsuda M, Hayashi H, Sugiura Y, Sugiyama T. 2015. The association between risk factors and time of onset for thrombocytopenia in Japanese patients receiving linezolid therapy: a retrospective analysis. *J Clin Pharm Ther* 40:279–284. <https://doi.org/10.1111/jcpt.12260>.
46. Takahashi Y, Takesue Y, Nakajima K, Ichiki K, Tsuchida T, Tatsumi S, Ishihara M, Ikeuchi H, Uchino M. 2011. Risk factors associated with the development of thrombocytopenia in patients who received linezolid therapy. *J Infect Chemother* 17:382–387. <https://doi.org/10.1007/s10156-010-0182-1>.
47. Zhou ZY, Zhao XQ, Shan BZ, Zhu J, Zhang X, Tian QF, Chen DF, Jia TH. 2014. Efficacy and safety of linezolid in treating gram-positive bacterial infection in the elderly: a retrospective study. *Indian J Microbiol* 54:104–107. <https://doi.org/10.1007/s12088-013-0422-z>.
48. Nukui Y, Hatakeyama S, Okamoto K, Yamamoto T, Hisaka A, Suzuki H, Yata N, Yotsuyanagi H, Moriya K. 2013. High plasma linezolid concentration and impaired renal function affect development of linezolid-induced thrombocytopenia. *J Antimicrob Chemother* 68:2128–2133. <https://doi.org/10.1093/jac/dkt133>.
49. French G. 2003. Safety and tolerability of linezolid. *J Antimicrob Chemother* 51(Suppl 2):ii45–ii53. <https://doi.org/10.1093/jac/dkg253>.
50. Narita M, Tsuji BT, Yu VL. 2007. Linezolid-associated peripheral and optic neuropathy, lactic acidosis, and serotonin syndrome. *Pharmacotherapy* 27:1189–1197. <https://doi.org/10.1592/phco.27.8.1189>.

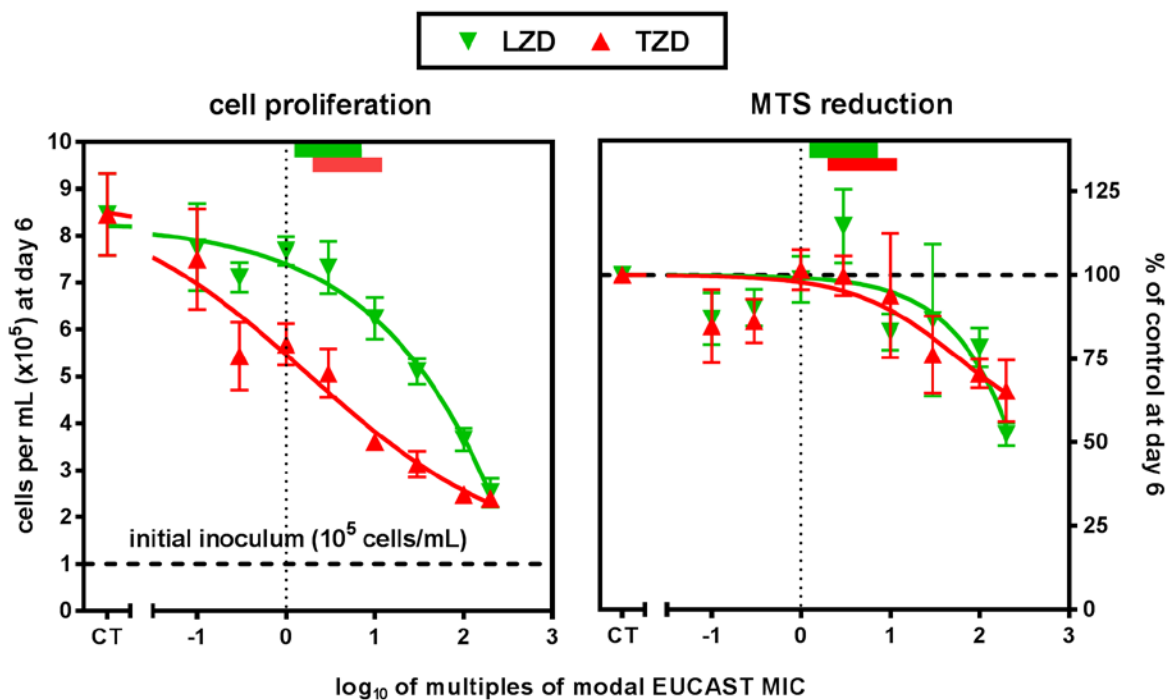
51. Metaxas EI, Falagas ME. 2009. Update on the safety of linezolid. *Expert Opin Drug Saf* 8:485–491. <https://doi.org/10.1517/14740330903049706>.
52. Vinh DC, Rubinstein E. 2009. Linezolid: a review of safety and tolerability. *J Infect* 59(Suppl 1):S59–S74. [https://doi.org/10.1016/S0163-4453\(09\)60009-8](https://doi.org/10.1016/S0163-4453(09)60009-8).
53. Garrabou G, Soriano A, Pinos T, Casanova-Molla J, Pacheu-Grau D, Moren C, Garcia-Arumi E, Morales M, Ruiz-Pesini E, Catalan-Garcia M, Milisenda JC, Lozano E, Andreu AL, Montoya J, Mensa J, Cardellach F. 2017. Mitochondrial toxicity of linezolid in blood cells and skin nerve fibers: influence of mitochondrial genetics. *Antimicrob Agents Chemother* 61:e00542-17. <https://doi.org/10.1128/AAC.00542-17>.
54. Hutchinson DK. 2003. Oxazolidinone antibacterial agents: a critical review. *Curr Top Med Chem* 3:1021–1042. <https://doi.org/10.2174/1568026033452195>.
55. Sciotti RJ, Pliushchev M, Wiedeman PE, Balli D, Flamm R, Nilius AM, Marsh K, Stolarik D, Jolly R, Ulrich R, Djuric SW. 2002. The synthesis and biological evaluation of a novel series of antimicrobials of the oxazolidinone class. *Bioorg Med Chem Lett* 12:2121–2123. [https://doi.org/10.1016/S0960-894X\(02\)00352-9](https://doi.org/10.1016/S0960-894X(02)00352-9).
56. Dranka BP, Hill BG, Darley-Usmar VM. 2010. Mitochondrial reserve capacity in endothelial cells: the impact of nitric oxide and reactive oxygen species. *Free Radic Biol Med* 48:905–914. <https://doi.org/10.1016/j.freeradbiomed.2010.01.015>.
57. Brand MD, Nicholls DG. 2011. Assessing mitochondrial dysfunction in cells. *Biochem J* 435:297–312. <https://doi.org/10.1042/BJ20110162>.
58. Vesce S, Jekabsons MB, Johnson-Cadwell LI, Nicholls DG. 2005. Acute glutathione depletion restricts mitochondrial ATP export in cerebellar granule neurons. *J Biol Chem* 280:38720–38728. <https://doi.org/10.1074/jbc.M506575200>.
59. Choi SW, Gerencser AA, Nicholls DG. 2009. Bioenergetic analysis of isolated cerebrocortical nerve terminals on a microgram scale: spare respiratory capacity and stochastic mitochondrial failure. *J Neurochem* 109:1179–1191. <https://doi.org/10.1111/j.1471-4159.2009.06055.x>.
60. Mosmann T. 1983. Rapid colorimetric assay for cellular growth and survival: application to proliferation and cytotoxicity assays. *J Immunol Methods* 65:55–63. [https://doi.org/10.1016/0022-1759\(83\)90303-4](https://doi.org/10.1016/0022-1759(83)90303-4).
61. Marroquin LD, Hynes J, Dykens JA, Jamieson JD, Will Y. 2007. Circumventing the Crabtree effect: replacing media glucose with galactose increases susceptibility of HepG2 cells to mitochondrial toxicants. *Toxicol Sci* 97:539–547. <https://doi.org/10.1093/toxsci/kfm052>.
62. Eakins J, Bauch C, Woodhouse H, Park B, Bevan S, Dilworth C, Walker P. 2016. A combined in vitro approach to improve the prediction of mitochondrial toxicants. *Toxicol In Vitro* 34:161–170. <https://doi.org/10.1016/j.tiv.2016.03.016>.
63. Zhou CC, Swaney SM, Shinabarger DL, Stockman BJ. 2002. 1H nuclear magnetic resonance study of oxazolidinone binding to bacterial ribosomes. *Antimicrob Agents Chemother* 46:625–629. <https://doi.org/10.1128/AAC.46.3.625-629.2002>.
64. Colca JR, McDonald WG, Waldon DJ, Thomasco LM, Gadwood RC, Lund ET, Cavey GS, Mathews WR, Adams LD, Cecil ET, Pearson JD, Bock JH, Mott JE, Shinabarger DL, Xiong L, Mankin AS. 2003. Cross-linking in the living cell locates the site of action of oxazolidinone antibiotics. *J Biol Chem* 278:21972–21979. <https://doi.org/10.1074/jbc.M302109200>.
65. Lodise TP, Bidell MR, Flanagan SD, Zasowski EJ, Minassian SL, Prokocimer P. 2016. Characterization of the haematological profile of 21 days of tedizolid in healthy subjects. *J Antimicrob Chemother* 71:2553–2558. <https://doi.org/10.1093/jac/dkw206>.
66. Fang E, Munoz KA, Prokocimer P. 2017. Characterization of neurologic and ophthalmologic safety of oral administration of tedizolid for up to 21 days in healthy volunteers. *Am J Ther* 24:e227–e233. <https://doi.org/10.1097/MJT.0000000000000534>.
67. Shorr AF, Lodise TP, Corey GR, De Anda C, Fang E, Das AF, Prokocimer P. 2015. Analysis of the phase 3 ESTABLISH trials of tedizolid versus linezolid in acute bacterial skin and skin structure infections. *Antimicrob Agents Chemother* 59:864–871. <https://doi.org/10.1128/AAC.03688-14>.
68. Yuste JR, Berto J, Del Pozo JL, Leiva J. 2017. Prolonged use of tedizolid in a pulmonary non-tuberculous mycobacterial infection after linezolid-induced toxicity. *J Antimicrob Chemother* 72:625–628. <https://doi.org/10.1093/jac/dkw484>.
69. Boak LM, Rayner CR, Grayson ML, Paterson DL, Spelman D, Khumra S, Capitano B, Forrest A, Li J, Nation RL, Bulitta JB. 2014. Clinical population pharmacokinetics and toxicodynamics of linezolid. *Antimicrob Agents Chemother* 58:2334–2343. <https://doi.org/10.1128/AAC.01885-13>.
70. Cooperstein SJ, Lazarow A. 1951. A microspectrophotometric method for the determination of cytochrome oxidase. *J Biol Chem* 189:665–670.
71. Lowry OH, Rosebrough NJ, Farr AL, Randall RJ. 1951. Protein measurement with the Folin phenol reagent. *J Biol Chem* 193:265–275.
72. Berridge MV, Herst PM, Tan AS. 2005. Tetrazolium dyes as tools in cell biology: new insights into their cellular reduction. *Biotechnol Annu Rev* 11:127–152. [https://doi.org/10.1016/S1387-2656\(05\)11004-7](https://doi.org/10.1016/S1387-2656(05)11004-7).
73. Cory AH, Owen TC, Barltrop JA, Cory JG. 1991. Use of an aqueous soluble tetrazolium/formazan assay for cell growth assays in culture. *Cancer Commun* 3:207–212.
74. Agilent Technologies. 2017. Agilent Seahorse XF Cell Mito stress test kit user guide kit 103015-100. Agilent Technologies, Inc, Santa Clara, CA. http://www.agilent.com/cs/library/usermanuals/Public/XF_Cell_Mito_Stress_Test_Kit_User_Guide.pdf.
75. Lemaire S, Van Bambeke F, Appelbaum PC, Tulkens PM. 2009. Cellular pharmacokinetics and intracellular activity of torezolid (TR-700): studies with human macrophage (THP-1) and endothelial (HUVEC) cell lines. *J Antimicrob Chemother* 64:1035–1043. <https://doi.org/10.1093/jac/dkp267>.
76. Tulkens P, Trouet A. 1978. The uptake and intracellular accumulation of aminoglycoside antibiotics in lysosomes of cultured rat fibroblasts. *Biochem Pharmacol* 27:415–424. [https://doi.org/10.1016/0006-2952\(78\)90370-2](https://doi.org/10.1016/0006-2952(78)90370-2).

Mitochondrial Alterations (Inhibition of Mitochondrial Protein Expression, Oxidative Metabolism and Ultrastructure) Induced by Linezolid and Tedizolid at Clinically-relevant Concentrations in cultured Human HL-60 promyelocytes and THP-1 monocytes

Tamara V. Milosevic, Valéry L. Payen, Pierre Sonveaux, Giulio G. Muccioli, Paul M. Tulkens, and Françoise Van Bambeke

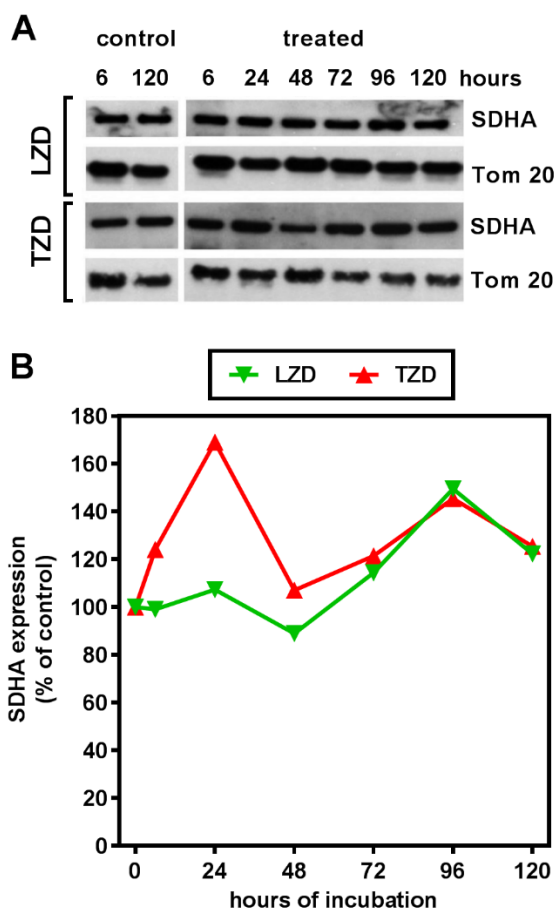
SUPPLEMENTAL MATERIAL

Figure S1

**Caption to Figure S1**

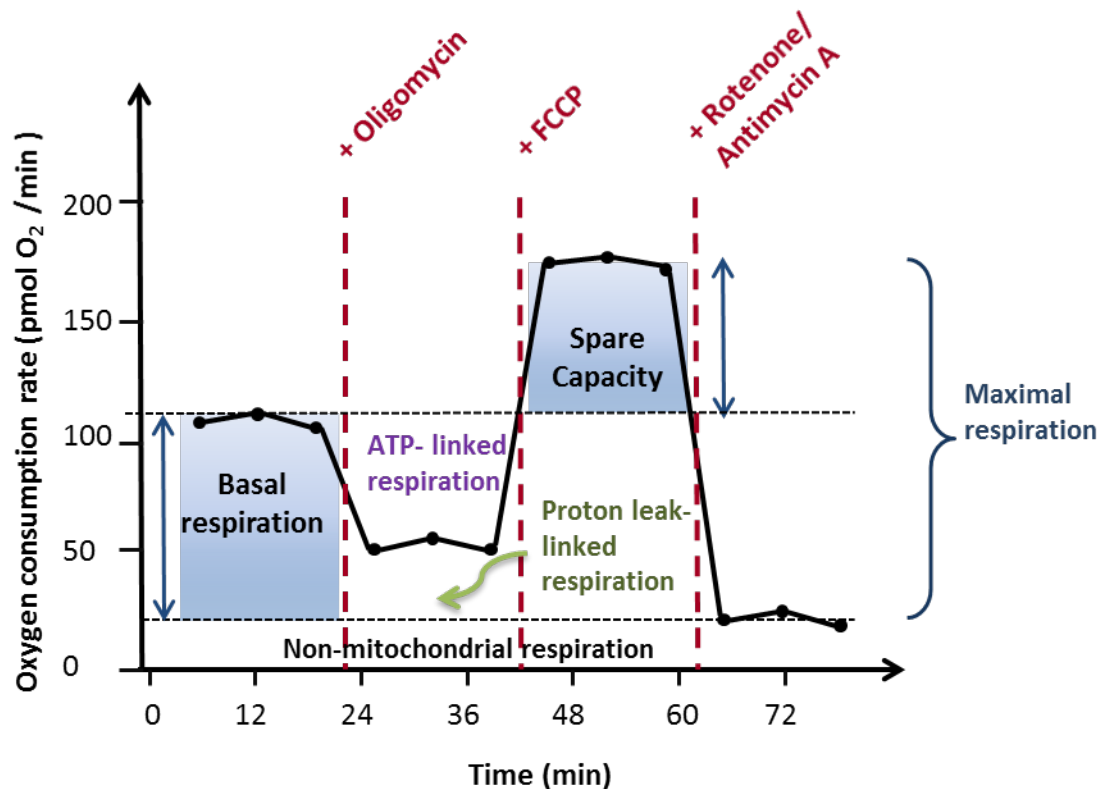
Influence of increasing concentrations of linezolid (LZD) or tedizolid (TZD) on cell number and global oxidoreductive metabolic activity of HL-60 promyelocytes incubated for 144 h in the absence (CT [control; vehicle only]) or presence of increasing oxazolidinone concentrations (0.2 to 400 mg/L for linezolid; 0.025 to 50 mg/L for tedizolid). For both panels, data are shown as means \pm SD of triplicates in a single experiment and are plotted against oxazolidinone concentrations expressed as \log_{10} of multiples of their respective modal MIC against *S. aureus* in EUCAST database [1] (LZD, 2 mg/L; TZD, 0.25 mg/L; vertical thin dotted line). Colored rectangles on the top of the graph indicate the typical C_{\min} to C_{\max} ranges of total serum concentrations values commonly observed at equilibrium in humans receiving conventional doses of either drug (LZD [green], 2.5 to 15 mg/L; TZD [red], 0.5 to 3 mg/L). **Left:** cell counts (the horizontal thick dotted line shows the value of the initial inoculum [day 0]). The concentrations achieving 50% inhibition of growth were for LZD 74 x MIC (148 mg/L; 438 μ M) and for TZD 5 x MIC (1.25 mg/L; 3.4 μ M). **Right:** MTS reduction normalized to cell number for each sample (in % of control [vehicle] at day 6; thick horizontal dotted line).

Figure S2

**Caption to Figure S2**

Influence of increasing time of exposure of HL-60 promyelocytes to linezolid (LZD; 15 mg/L) and tedizolid (TZD; 3 mg/L) at C_{max} on SDHA (one the 4 subunits of succinate dehydrogenase [encoded by the nuclear DNA]) expression. **A**, Western blots of SDHA and of Tom 20 (used for normalization) of mitochondrial protein fractions. **B**, quantitative measurements of band densities ratios (SDHA to Tom 20) expressed as percentage of the control value (no oxazolidinone added) and plotted against the time of exposure to the corresponding oxazolidinone.

Figure S3

**Caption to Figure S3**

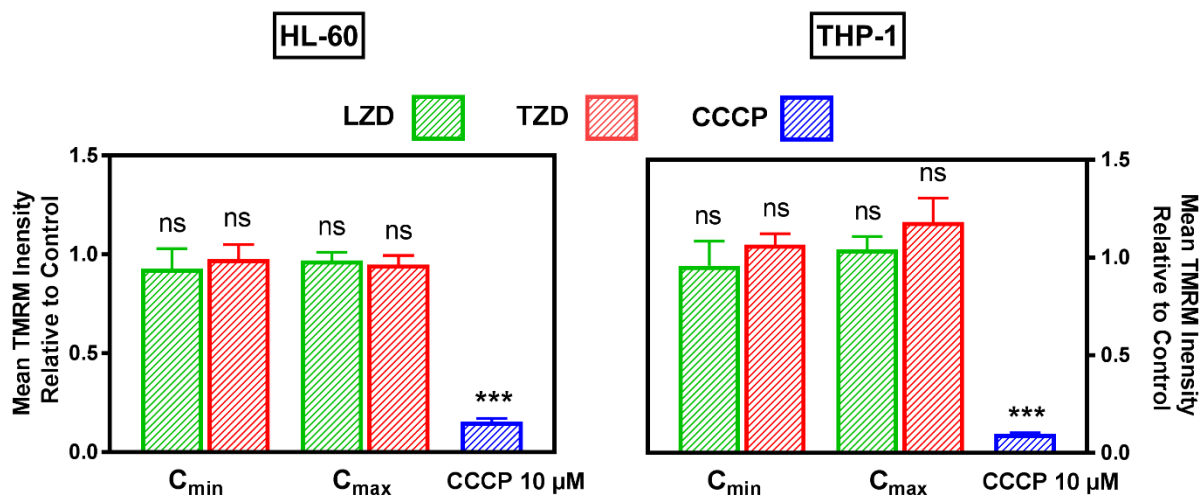
Procedure for measuring parameters of mitochondrial function from the direct measurements of oxygen consumption rate (OCR) of cells by means of successive addition of specific inhibitors using the Agilent Seahorse XF Cell Mito Stress Test Kit®. Basal OCR is measured first in the absence of any inhibitor. The decrease of OCR observed upon addition of oligomycin (ATP synthase inhibitor) allows to measure ATP-linked respiration. Addition of carbonyl cyanide-4-(trifluoromethoxy)phenylhydrazone (FCCP), a proton ionophore, uncouples oxygen consumption from ATP production, forcing the electron transport chain to work at its maximal rate and allowing maximal OCR measurement. The spare capacity is then the difference between the maximal and the basal OCR. Further addition of rotenone and antimycin A (complex I and III inhibitors, respectively), fully inhibits mitochondrial oxygen consumption allowing non-mitochondrial OCR measurement (Figure and text adapted from [2,3]). See Table S1 for further definition and mechanistic explanation of the successive rates of respiration measured.

Table S1

Definition and underlying biological mechanisms of the successive OCR measured with the Agilent Seahorse XF Cell Mito Stress Test Kit. Reproduced from (3) with permission.

Rate	Definition	What sets the rate of respiration
Basal respiration	Respiration used to meet the endogenous ATP demand of the cell and drive proton leak pathways.	The basal rate of respiration can be set by the rate of ATP utilization, substrate availability and oxidation, or proton leak.
ATP-linked respiration	Respiration that is sensitive to oligomycin can estimate the respiration that is used to drive mitochondrial ATP synthesis.	The rate of ATP-linked respiration is largely set by the ATP demand of the cell. It can also be set by substrate supply and oxidation, particularly if there is mitochondrial dysfunction.
Proton leak	Oxidative phosphorylation is incompletely coupled, as protons can leak across the inner membrane independently of ATP synthase. This leak can regulate several physiological processes.	The magnitude of oligomycin-insensitive respiration is mostly set by proton leak. Based on the experimental model and context, high leak may indicate mitochondrial injury or a normal physiological response.
Maximal respiration	A titrated amount of FCCP can estimate the maximum rate of respiration. In response to protonophore addition, substrate oxidation and respiratory chain activity increase in an attempt to maintain mitochondrial membrane potential.	The rate of maximal respiration is mostly set by substrate supply and oxidation. This includes substrate transport across the plasma and mitochondrial membranes as well as rate-controlling metabolic enzymes. Changes may also reflect altered mitochondrial biogenesis or cristae density.
Reserve/Spare respiratory capacity	The reserve (or spare respiratory) capacity is the difference between the basal and maximal respiration. Broadly, this indicates the ability of a cell to meet an increased energy demand.	As a function of both the basal and maximal respiration rate, each of the factors that affect rates can also affect the reserve capacity.
Non-mitochondrial respiration	Mitochondrial respiration is blocked upon addition of electron chain inhibitors such as rotenone (Complex I) and antimycin A (Complex III).	Changes may indicate differential cell number if parallel differences appear elsewhere. In some systems, cytoplasmic oxidases are relevant (e.g. hematopoietic cells, high ROS/RNS).

Figure S4



Caption to Figure S4

Absence of influence of linezolid (LZD) and tedizolid (TZD) on mitochondrial membrane potential. HL-60 promyelocytes and THP-1 monocytes were incubated during 48 h and 72 h respectively with linezolid or tedizolid at two concentrations corresponding to their C_{min} and C_{max} (linezolid: 2.5 and 15 mg/L; tedizolid: 0.5 and 3 mg/L), then incubated with tetramethyl rhodamine methyl ester (TMRM) at 37°C, and subjected to fluorescence-activated cell sorting (FACS). Carbonyl cyanide m-chlorophenyl hydrazine (CCCP) at 10 µM is used as a positive control. Results are shown as means ± SEM of TMRM intensities (relative to control) recorded in the FACS analyzer, from three experiments (n=3). Statistical analysis: one-way ANOVA with Tukey-Kramer multiple comparisons test (comparing all pairs of columns) (ns: p > 0.05, * p < 0.05, ** p < 0.01, *** p < 0.01).

REFERENCES

1. **Anonymous.** Antimicrobial wild type distributions of microorganisms. <https://mic.eucast.org/Eucast2/> , European Committee on Antimicrobial Susceptibility Testing (EUCAST); last updated: 2017, last accessed: July 1, 2017
2. **Anonymous.** Agilent Seahorse XF Cell Mito Stress Test Kit User Guide Kit 103015-100. http://www.agilent.com/cs/library/usermanuals/Public/XF_Cell_Mito_Stress_Test_Kit_User_Guide.pdf , Agilent Technologies, Inc., Santa Clara, CA; last updated: 2017, last accessed: July 2, 2017
3. **Divakaruni, A. S., A. Paradyse, D. A. Ferrick, A. N. Murphy, and M. Jastroch.** 2014. Analysis and interpretation of microplate-based oxygen consumption and pH data. *Methods Enzymol.* **547**:309-354.PMID: PM:25416364.